Synthesis of Amino Functional Monomers via Controlled Radical Polymerization. Solution Properties of Thermo-Responsive Polymers With Controlled Architectures.

Xeniya Savelyeva

Department of Chemical Engineering, McGill University
Montréal, QC, Canada

August, 2014

A thesis submitted to McGill University in partial fulfilment of the requirements of the degree of Master of Engineering

Acknowledgments

The thesis could not have been completed without the support I have received from many people. I would like to give a very special thanks to the following people.

To my advisor, Milan Maric. I have been very fortunate to meet him during my undergraduate study at McGill, and then joining his research group. I thank him for his patient guidance, enthusiastic encouragement and useful critiques of this research work. He has been my mentor and a role-model for scholarly excellence.

To my amazing lab group and my office mates, Chi Zhang and Stacey Lee, for their shared knowledge and support through the obstacles of research.

To our former graduate student, Benoit Lessard, for being my mentor and teaching me all the "hands-on" and laboratory techniques required for my first project.

To the technical staff of the Department of Chemical Engineering, McGill University. In particular, I thank Andrew Golsztajn for his help in the analytical laboratory, Lou Cusmich, Melanie Gorman and Frank Caporuscio for their help in the workings of the building and the proper safety protocol, which helped to reduce the risk of accidents in the laboratory.

To the funding agencies, which made this research possible: Eugenie Ulmer Lamothe (EUL) Scholarship and Natural Science Engineering Research Council of Canada Discovery Grant.

To Prof. Bruce Lennox in Department of Chemistry, McGill University, for allowing to use his lab facilities and UV-Vis Spectrometer.

To the students I have supervised, Pavlo, Lucia and David. You showed me the joys of teaching.

To my friends, Anna and Kate, for their support and for being there for me.

To my parents, my brother and the rest of my family. I am grateful for your constant support and encouragement throughout my study.

To anyone that I may have forgotten. Thank you as well.

Table of Contents

List of Figures

List of Tables

Contribution of Author

The thesis' format is manuscript based, and it contains two manuscripts where I, Xeniya Savelyeva, am the first author and have done the majority of the work.

The first manuscript is presented as chapter 2 in the thesis: **"Pyrrolidone-Functional Smart Polymers via Nitroxide Mediated Polymerization".** As a contribution to this manuscript, I performed the majority of the synthesis, characterization and data analysis. The body of the manuscript was initially written by me. My supervisor Prof. Milan Maric performed the final editing.
Published: (Savelyeva, X. and Marić, M.. *J. Polym. Sci. Part A: Polym. Chem.* 52 (14) **2014**, 2011-2024)

The second manuscript is presented as chapter 3 in the thesis: **"Using Controlled Radical Polymerization to Confirm the Lower Critical Solution Temperature of a *N*-(Alkoxyalkyl) Acrylamide Polymers in Aqueous Solution".** As a contribution to this manuscript, I performed the majority of the synthesis, characterization and data analysis. The body of the manuscript was initially written by me. My supervisor Prof. Milan Maric performed the final editing.
Submitted: *J. Polym. Sci. Part A: Polym. Chem.* (Manuscript # JPOL-A-14-0583, July 18, 2014)

Abstract

Controlled radical polymerization (CRP) techniques has allowed the synthesis of numerous polymeric materials with comparable control to that of true "living" techniques without the need for stringent manipulation techniques. The control over chain length, dispersity and composition is desirable in many fields, such as stimuli-responsive (temperature or pH) drug carriers. These thermoresponsive polymers in aqueous media are often characterized by lower critical solution temperature (LCST) behavior, where the polymer becomes insoluble with temperature increases. The LCST can be tuned by the structural features of the constituent monomer, molecular weight, molecular weight distribution and copolymerization with other monomers. Narrow molecular weight distribution is the key factor determining the sharpness needed for determining the LCST, which is often exemplified by the cloud point temperature (CPT). Using CRP techniques, specifically nitroxide mediated polymerization (NMP), with an alkoxyamine unimolecular initiator, 2-([*tert*-butyl[1-(diethoxyphosphoryl)-2,2-dimethylpropyl]amino]oxy)-2-methylpropanoic acid (BlocBuilder) and an additional free nitroxide (SG1), the effect of controlling comonomer (9-(4-vinylbenzyl)-9H-carbazole (VBK)) on polymerization kinetics of *N*-(2-methacryloyloxyethyl) pyrrolidone (MAEPYR) and the effect of final copolymer composition on CPT was studied. Adding at least 5 mol% VBK, the dispersity Đ of the poly(MAEPYR-*stat*-VBK) copolymers was below 1.4. The CPT decreased from 59.0 °C to 49.7 °C with addition of only 1 mol% of VBK in the copolymer, and it can be further fine-tuned by changing the solution concentration and the heating rate. Another CRP technique, reversible addition fragmentation chain-transfer polymerization (RAFT), was applied to homopolymerization of *N*-(3-methoxypropyl) acrylamide (MPAM) to yield well-defined polymers (with $\overline{M_n}$ = 14.3 - 25.2 kg mol^{-1} and low Đ ~ 1.17 - 1.47) needed for precise determination of CPT. Thermoresponsive behaviour of poly(MPAM) in aqueous media revealed CPTs between 73 and 92 °C, unlike other literature reports where the polymers, synthesized by conventional radical polymerization, showed conflicting results regarding their LCST-behavior.

Abrégé

Des techniques de polymérisation radicalaire contrôlée ont permis la synthèse de nombreux matériaux polymeres avec un contrôle comparable à celui des vraies techniques “vivantes” sans la nécessité de manipulations strictes. Le contrôle de la longueur de la chaîne, la polydispersité et la composition est souhaitable dans de nombreux domaines, tels que des vecteurs de médicaments stimuli-sensibles (activés par la température ou le pH). Ces polymères sensibles à la température dans des milieux aqueux sont souvent caractérisés par la température inférieure critique de la solution (LCST), dans lesquels le polymère devient insoluble avec une augmentation de la température. La LCST peut être réglée par les caractéristiques structurelles du monomère: la masse moléculaire, la distribution de la masse moléculaire et la copolymérisation avec d'autres monomères. Une distribution de la masse moléculaire étroite est le facteur clé qui détermine la précision nécessaire pour déterminer la LCST, aussi appelée température de point de trouble (CPT). En utilisant des techniques de CRP, en particulier la polymérisation médiée par nitroxyde (NMP), avec l'initiateur alcoxyamine, l’acide 2-([*tert*-butyl[1-(diethoxyphosphoryl)-2,2-dimethylpropyl]amino]oxy)-2-methylpropanoic (BlocBuilder) et un nitroxyde libre supplémentaire (SG1), l'effet du comonomère contrôle (9-(4-vinylbenzyl)-9H-carbazole (VBK)) sur la cinétique de polymérisation de *N*-(2-methacryloyloxyethyl) pyrrolidone (MAEPYR) et l'effet de la composition de copolymère final de CPT a été étudiée. L’addition au moins 5 mol% VBK, la dispersité de la poly(MAEPYR-*stat*-VBK) copolymère était inférieure à 1.4. Le CPT a diminué de 59.0 ºC à 49.7 ºC avec addition de seulement 1 mol% de VBK dans le copolymère, et elle peut encore être affinée en changeant la concentration de la solution et la taux de chauffe. Une autre technique de CRP, la polymérisation radicalaire contrôlée par transfert de chaîne réversible par addition-fragmentation (RAFT), a été appliquée à l'homopolymérisation du *N*-(3-methoxypropyl) acrylamide (MPAM) pour donner des polymères bien définis (avec $\overline{M_n}$ = 14.3 à 25.2 kg mol^{-1}et Đ ~ 1.17 à 1.47) nécessaires pour la détermination précise de la CPT. Le comportement thermosensible du poly(MPAM) dans des milieux aqueux a révélé un CPT entre 73 et 92 ºC, contrairement à ce qu’il a déjà été rapporté dans la littérature où les polymères, synthétisés par polymérisation radicalaire classique, ont montrés des résultats contradictoires quant à leur comportement vis-à-vis la LCST.

1. General Introduction

1.1 Controlled/Living Radical Polymerization

A living polymerization can be regarded as the one proceeding without chain transfer and termination; hence, the polymeric molecules 'live' for an indefinite period of time. Szwarc in his work of 1956 introduced the concept of living polymerization which allowed the control of precise predetermined masses, compositions and functionalities.[1] The drawback of the method is its inability to polymerize a wide range of monomers; only the ones whose structures could enhance the stability of the ion (including dienes, styrene, (meth)acrylates, acrylonitriles, and others[2] could be polymerized. Also, due to the presence of highly reactive ions, inert experimental conditions are required, which include the absence of moisture, oxygen or any other impurities since they are effective termination agents.[2, 3]

Free radical polymerization is one of the most popular techniques used in industry.[4] It is advantageous due to its low sensitivity to impurities, and moderate reaction conditions. Its main disadvantage is lack of the control over the molecular weight and molecular weight distribution, thus, making it difficult to synthesize polymers with controlled microstructures.

The living anionic and cationic polymerizations were the only available methods to obtain polymers with structural homogeneity until the mid-1980s when the concept of controlled/living radical polymerization (CRP) was introduced. It brings in the concepts of both free radical and ionic polymerizations: it is as easy to use as free radical polymerization, and it provides a high control of microstructure like ionic polymerization does. CRP, although not a true living polymerization, relies on reversible activation/deactivation of the chain radicals to suppress termination to a certain extent.[5] The chains are free to propagate once activated as in a conventional free radical polymerization, which makes CRP or reversible-deactivation polymerizations *quasi living*[5] due to reduced probability of chain transfer and termination. Three CRP methods have been actively investigated: nitroxide mediated polymerization (NMP), atom transfer radical polymerization (ATRP), and reversible addition-fragmentation chain transfer (RAFT) polymerization. Most of the research work focuses on the improvement of these systems, since the choice of the technique depends on the adaptability of the controlling agent to a monomer type. Newer types of CRP, however, constantly being developed, including cobalt-mediated polymerization[6], reverse iodine transfer polymerization (RITP)[7], organotelluriummediated living radical polymerization (TERP)[8], organostibine-mediated living radical polymerization (SBRP)[9, 10], and others. The three most common techniques, NMP, ATRP and RAFT, are explained in further details.

1.1.1 Nitroxide-Medicated Polymerization (NMP)

NMP was the first CRP technique that was discovered by Solomon, Rizzardo and Cacioli during the mid-1980s. Initially, it was limited to polymerization of styrenic compounds only; however, as new initiators have been developed, the range of polymerizable monomers by NMP now includes not only styrene and related styrenic monomers, but also acrylates, acrylamides, acrylonitriles and dienes.[2] NMP has difficulties in controlling polymerization of methacrylates; however, control over the polymerization increases if a small amount of comonomer, e.g. styrene, is added to the reaction mixture.[2, 11] The polymerization experiments can be done in bulk or using a solvent, and recently NMP was extended to dispersed aqueous media (eg. emulsion/miniemulsion) which facilitates its industrial applications.[12, 13] NMP does not require any rigorous purification conditions or post-polymerization treatments to obtain well-defined polymers; therefore, small amounts of impurities are tolerated, which makes NMP a relatively robust technique.[14] Quite a few mediators are available commercially nowadays, and even more are discovered in order to expand the range of polymerizable monomers.

1.1.2 Reversible Addition-Fragmentation Chain Transfer Polymerization (RAFT)

The second method is free-radical polymerization with reversible chain transfer. The range of polymerizable monomers includes styrene, (meth)acrylates, acrylonitriles, (meth)acrylamides with no limitations for temperature (ambient to 140 °C) or solvent (both organic and aqueous) used for the reaction.[2, 15] RAFT is capable of synthesizing polymers with controlled architectures, and the reaction is quite tolerant to the presence of impurities.[2] The RAFT polymerization uses a dithioester chain transfer agent, thus polymer chains carry this residue, which is very promising for a subsequent end-group-functionalization.[16-20] One of the disadvantages is that dithioester groups may have some odours and colors associated with them; however, there are simple and cost effective post-polymerization treatments which can remove the color from the RAFT polymers.[2, 21]

1.1.3 Atom Transfer Radical Polymerization (ATRP)

Lastly, the third most popular CRP method is polymerization with reversible deactivation by atom transfer. The difference between ATRP and NMP consists of the reversible termination by ligand coupling to a metal complex in the ATRP process. In addition to its advantage of control, ATRP is compatible with many monomers and functional groups and, unlike ionic polymerization process, ATRP is quite tolerant to the presence of impurities.[2, 22] It is a catalytic process and can be mediated by many redox-active transition metal complexes.[22] All necessary ATRP reagents are commercially available.[2] One of the disadvantages is that the transition metal catalyst must often be removed and the polymers tend to be discolored.[2]

1.2 Stimuli-Responsive Polymers

CRP methods were developed to afford polymers with tailored microstructures, which was done previously only by living methods. The control over the molecular weight and distribution is required for developing a new generation of intelligent or "smart" materials used in many applications. These stimuli-responsive materials receive or process a stimulus and respond by producing a useful, and in most cases reversible, effect. Such intelligent materials include, but are not limited to: piezolelectric materials, thermo-responsive materials, pH-sensitive materials, ultraviolet-(UV) sensitive materials, smart polymers, hydrogels, smart catalysts, and shape memory alloys.

Temperature sensitive polymers exhibit lower critical solution temperature (LCST), which is sometimes referred as cloud point temperature (CPT), the temperature at which polymers undergo a phase separation with temperature increases.[5] These polymers, when synthesized by conventional radical polymerization, are often characterized by broad transitions and poorly defined LCSTs. Controlled polymerization via robust CRP methods is of high interest since the narrow molecular weight distribution is essential for sharp transition and fast response to temperature changes.

The balance between the hydrophobic and hydrophilic forces determines the solution properties of the polymer. The phase transition can be adjusted by polymer's backbone: e.g. poly(*N*-isopropylacrylamide) has a lower[23] LCST than poly(*N*-isopropylmethacrylamide). The higher LCST of the later one can be explained by the constraint of hydrogen bonding due to rotation of methyl groups.[23] Similarly, poly(2-*N*-morpholinoethyl acrylate) was completely water soluble for the range of temperature studied (20-95 °C) and poly(2-*N*-morpholinoethyl methacrylate) had an LCST at about 37°C.[24] Therefore, by tailoring the monomer unit structure it is possible to influence the phase transition of polymers.

1.3 Objectives

The objective of the study was to investigate the stimuli-responsive behavior of nitrogen-containing polymers synthesized by CPR methods. Many known stimuli-responsive polymers are poly(methacrylates) and poly(acrylamides). The methacrylate monomer with a pyrrolidone functionality, *N*-(2-methacryloyloxyethyl) pyrrolidone (MAEPYR), has been polymerized in a controlled manner previously using RAFT and conventional radical polymerization, but not by NMP. Potential applications of pyrrolidone-containing polymers urge us to apply CRP methods for controlled synthesis of the polymers with tailored microstructure and narrow molecular weight distribution, which are required for precise determination of CPT (Chapter 2). The phase behaviour for the acrylamide monomer, *N*-(3-methoxypropyl) acrylamide (MPAM), is inconclusive since the polymer has been polymerized by conventional free radical polymerization only. The objective of the second part of the thesis was to apply CRP methods for controlled synthesis of MPAM polymers and hopefully unambiguous determination of CPT (Chapter 3).

2. Pyrrolidone-Functional Smart Polymers via Nitroxide Mediated Polymerization.

Nitroxide mediated polymerization (NMP) of *N*-(2-methacryloyloxyethyl) pyrrolidone (MAEPYR) with 2-([*tert*-butyl[1-(diethoxyphosphoryl)-2,2-dimethylpropyl]amino]oxy)-2-methylpropanoic acid (BlocBuilder) initiator and *N*-tert-butyl-*N*-[1-diethylphosphono-(2,2-dimethylpropyl)] (SG1) nitroxide permitted controlled synthesis of poly(*N*-(2-methacryloyloxyethyl)-pyrrolidone-*stat*-9-(4-vinylbenzyl)-9H-carbazole) (poly(MAEPYR-*stat*-VBK)) statistical copolymers. With at least 5 mol% VBK, the dispersity Đ of the copolymers was below 1.4 at conversions less than 50%. At conversions higher than 50%, and at lower VBK feed content, there was a significant amount of termination reactions, which broadened the molecular weight distribution of the final polymers (Đ = 1.4 - 2.3). The MAEPYR-rich statistical copolymers were subsequently tested for thermo-responsive behaviour in aqueous media. The cloud point temperatures (CPT) in aqueous solution were tuned by changing the VBK composition, solution concentration and heating rate, and the transitions were thermally reversible with partial loss of reversibility at higher heating rates. The CPT decreased from 59.0 °C to 49.7 °C with addition of only 1 mol% of VBK in the copolymer, and at more than 6 mol% VBK, the copolymer was water-insoluble.

2.1 Manuscript Introduction

A functional material that can respond to different external stimuli is a key towards developing a new generation of intelligent or "smart" materials. The response of such materials can be regarded as a change in shape, solubility, and surface characteristics[25], usually with an attendant reversibility. The stimuli for these transitions can be a change in temperature, pH[26], ionic strength[26], light[27] or presence of certain metabolic chemicals[28]. Materials that can undergo a phase transition in response to the changes in the metabolic variables of biological fluids, (temperature and/or pH) are of special interest[29] in a wide range of applications, such as drug delivery, biosensors, tissue engineering, coatings, textiles and optical systems. As the most widely used stimulus[30], temperature can be easily controlled and applied both *in vivo*[31, 32] and i*n vitro*[33, 34]. Many temperature sensitive polymers exhibit a lower critical solution temperature (LCST) in water, which is the critical point where a polymer becomes water-insoluble upon heating.[5] Poly(*N*-isopropylacrylamide) (PNIPAM) has become the most studied temperature-sensitive polymer, particularly since its LCST is near body temperature[23, 35-38].

The hydrophobic and hydrophilic moieties present in the chain determine the LCST of the phase transition.[30] The phase transition can be adjusted subtly by the changes in a monomer's structure. For instance, Cai and coworkers reported a decrease in cloud point temperature (CPT) of as much as 37 °C from the acrylic-based pyrrolidone functional homopolymers (CPT ≈ 66.5 °C, poly[*N*-(3-acryloyloxypropyl) pyrrolidone]) to the methacrylic-based pyrrolidone functional homopolymers (CPT ≈ 29.5 °C, poly[*N*-(3-methylacryloyloxypropyl) pyrrolidone]).[39] Poly(2-*N*-morpholinoethyl acrylate) (PMEA)) and poly(2-*N*-morpholinoethyl methacrylate) (PMEMA)) were analysed recently by our group for their phase transition behavior. PMEA was completely water soluble in the range of temperatures studied (20-95 °C); whereas PMEMA had a CPT at about 37 °C.[24] The higher CPT of the latter polymer can be explained by the constraint of hydrogen bonding due to rotation of the backbone methyl groups.[23] Poly(*N*-vinyl-pyrrolidone) (PVP) is another example where the subtle changes in the molecular structure affects the phase transition. PVP is soluble in aqueous solution over a wide range of temperature; however, its analogues, where the molecular structure was modified by addition of a hydrophobic spacer, were shown to have a LCST.[39, 40] Polymers with pyrrolidone functionalities are applied in biomedical research due to their water solubility[41, 42], biocompatibility[40-42], low toxicity[41], and coordination capacity[39, 40, 42]. PVP can also be used as a blood plasma substitute[41-44], food thickener[42], binding agent for drug delivery[40, 43], and inhibitor of hydrate formation[45, 46].

Polymer microstructure influences directly the polymer properties. In the case of temperature responsive polymers, the response to temperature changes is sharp for monodisperse samples, and it is less defined for polymers with broad molecular weight distributions.[39, 47-49] Various polymerization techniques, such as living ionic polymerization, have been developed to allow the synthesis of well-defined polymers with predictable molecular weight and precise microstructure. Ionic polymerization, however, requires very stringent reaction conditions since the presence of any impurity (e.g. air, moisture) will terminate the reaction. This is where controlled radical polymerization (CRP) becomes useful. It has moderate sensitivity to the impurities, like conventional radical polymerization, and it has pseudo "living" character as in ionic polymerization since termination reactions can be sufficiently suppressed for a significant portion of the polymerization. CRP techniques do not require rigorous purification conditions to obtain well-defined polymers; therefore, small amounts of impurities are tolerated.[50] Among various techniques currently used for CRP, reversible addition-fragmentation chain transfer polymerization (RAFT)[51-54], nitroxide mediated polymerization (NMP)[42, 55-57] and atom transfer radical polymerization (ATRP)[58, 59] are the most popular ones.[59]

MAEPYR monomer (Scheme 2-1) shares similar properties with *N*-vinylpyrrolidone (VP) due to the common pyrrolidone functionality. Hadjichristidis and co-workers have attempted to polymerize VP via NMP using 2,2,6,6-tetramethylpiperidinyl-1-oxy (TEMPO) nitroxide.[42, 43] The final polymers were obtained at low yields with high dispersity (1.7 - 2.2) mostly due to the prevalent termination reactions present at prolonged reaction times.[43] MAEPYR has been polymerized in a controlled manner previously using RAFT[39, 60] and conventional radical polymerization[61], but not by NMP. NMP does not require removal of metallic impurities, as in the case of ATRP, nor does it use sulphur-based chain transfer agents as in the case of RAFT. It is thus valuable to see if NMP's favourable characteristics can be used for a controlled synthesis of MAEPYR polymer without impeding phase transition properties in aqueous solution. However, to apply NMP via commercially available BlocBuilder (2-([*tert*-butyl[1-(diethoxyphosphoryl)-2,2-dimethylpropyl]amino]oxy)-2-methylpropanoic acid), the methacrylate must be copolymerized with a comonomer in order to decrease the average equilibrium constant to keep the polymerization controlled. Styrene and acrylonitrile are examples of the most commonly used controlling comonomers.[11, 62] Our group has found that 9-(4-vinylbenzyl)-9H-carbazole (VBK) (Scheme 2-1) can be used as a very effective controlling comonomer.[24, 63-67] The VBK units not only served to control the copolymerization with reduced amount of comonomer compared to styrene, but imparted fluorescent, electron-donating functionality into the copolymers and permitted tuning of the LCST due to its relative hydrophobicity.

In this study NMP with BlocBuilder (Scheme 2-1) was examined to yield MAEPYR-rich copolymers when using VBK as a controlling comonomer. The activity of the copolymers' chain end was assessed by reinitiating with a fresh batch of *N*,*N*-dimethylacrylamide (DMAA) (Scheme 2-1). The resulting statistical and block copolymers were solubilized in aqueous solutions and their CPTs were measured. The effect of copolymer composition, solution concentration, pH and the addition of poly(DMAA) block was studied and reported.

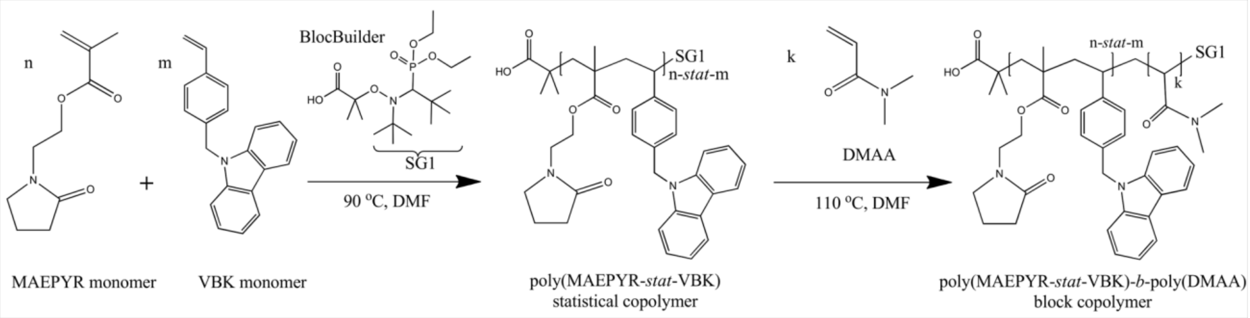

Scheme 2- 1 Synthetic route used to obtain poly(*N*-(2-methacryloyloxyethyl) pyrrolidone-*stat*-9-(4-vinylbenzyl)-9H-carbazole) (poly(MAEPYR-*stat*-VBK)) statistical copolymers by NMP using BlocBuilder initiator followed by the chain extension with *N*,*N*-dimethylacrylamide (DMAA) to form poly(*N*-(2-methacryloyloxyethyl) pyrrolidone-*stat*-9-(4-vinylbenzyl)-9H-carbazole)-*b*-poly(*N*,*N*-dimethylacrylamide) (poly(MAEPYR-*stat*-VBK)-*b*-poly(DMAA)) block copolymer.

2.2 Experimental Section

2.2.1 Materials

Calcium hydride (90-95%, reagent grade, Sigma Aldrich), basic alumina (Brockmann, type 1, 150 mesh, Sigma Aldrich), lithium bromide (ReagentPlus, ≥99%, Sigma Aldrich), 1-(2-hydroxyethyl)-2-pyrrolidone (98%, Sigma Aldrich), dimethyl sulfoxide (DMSO) (deuterated-d_6, 99%, Sigma Aldrich), methacryloyl chloride (97%, contains 200 ppm monomethyl ether hydroquinone as stabilizer, Sigma Aldrich), *N*,*N*-dimethylformamide (DMF, >95% certified ACS, and 99.5% HPLC grade, Acros Organics), ethyl ether anhydrous (>95%, BHT stabilized/certified ACS, Fisher Scientific), magnesium sulfate (anhydrous, certified powder, Fisher Scientific), sodium chloride (≥99.5, certified ACS, Fisher Scientific), sodium carbonate (anhydrous, ≥99.5, certified ACS, Fisher Scientific), and triethylamine (99 %, Fisher Scientific) were used as received. The deuterated chloroform ($CDCl_3$, >99%) was obtained from Cambridge Isotopes Laboratory and also used as received. Chloroform (>99%, reagent ACS grade, Fisher Scientific), and *N*,*N*-dimethylacrylamide (DMAA, 99%, contains 500 ppm monomethyl ether hydroquinone as stabilizer, Sigma Aldrich) were purified by passage through a column of 5 wt % calcium hydride relative to basic alumina and then stored in a sealed flask under a head of nitrogen in a fridge until needed. *N*-(2-methacryloyloxyethyl) pyrrolidone (MAEPYR) was synthesized according to the literature[60] with slight variations as noted below and stored in a sealed flask under a head of nitrogen in a refrigerator until needed. 9-(4-vinylbenzyl)-9H-carbazole (VBK) was synthesized according to the literature[68] and stored in a refrigerator away from the light source. 2-([*tert*-butyl[1-(diethoxyphosphoryl)-2,2-dimethylpropyl]amino]oxy)-2-methylpropanoic acid, also known as BlocBuilder (99%), was obtained from Arkema and used without further purification. [*tert*-butyl[1-(diethoxyphosphoryl)-2,2-dimethylpropyl]amino]oxidanyl, also known as SG1 (>85%), was kindly donated by Noah Macy of Arkema and used as received. 2-Cyano-2-propyl dodecyl trithiocarbonate (CPDTC) was obtained from Sigma Aldrich and used without further purification. 2,2'-azobisisobutyronitrile (AIBN, Vazo 67 from Du Pont) was recrystallized from methanol.

2.2.2 Monomer Synthesis

The esterification reaction was adopted from Cai et al.[60] with slight variations. A 125 ml 3-neck jacketed reactor, equipped with a stir bar, and a dropper column were used. Measured amounts of 1-(2-hydroxyethyl)-2-pyrrolidone (40.06 g, 0.31 mol), triethylamine (31.26 g, 0.31 mol) and anhydrous chloroform (35 ml) were added to the reactor and stirred well at 5 °C. The reaction mixture was purged with nitrogen for 20 minutes. Methacryloyl chloride (32.40 g, 0.31 mol) was diluted with anhydrous chloroform (40 ml), and then the mixture was added to the reactor drop-wise over a 1 hour period. The reaction was allowed to proceed for at least 10 hours at 10 °C. The nitrogen purge remained for the entirety of the reaction. For the purification, white ammonium salt was removed by vacuum filtration. The solution was first concentrated by rotary evaporation, and then extracted thrice using first 5 wt% Na_2CO_3 (200 ml), then saturated NaCl solution (100 ml) and deionized water (200 ml). The solution was dried under $MgSO_4$ (3 g), and concentrated by rotary evaporation to remove any solvent residuals. The monomer's structure was verified by nuclear magnetic resonance (^1H NMR) spectroscopy in deuterated chloroform and DMSO. The final yield was 14.7 g (24%).

^1H NMR (δ, in $CDCl_3$): 6.08 and 5.56 ppm (2H, $C\mathit{H}_2{=}CHCH_3$), 4.25 ppm (2H, $COOC\mathit{H}_2CH_2$), 3.56 ppm (2H, $COOCH_2C\mathit{H}_2$), 3.46 ppm (2H, $NCOCH_2CH_2C\mathit{H}_2$ in pyrrolidone ring), 2.35 ppm (2H, $NCOC\mathit{H}_2CH_2CH_2$ in pyrrolidone ring), 2.01 ppm (2H, $NCOCH_2C\mathit{H}_2CH_2$ in pyrrolidone ring), 1.91 ppm (3H, $CH_2{=}CHC\mathit{H}_3$).

2.2.3 Polymer Synthesis

General

All the copolymerizations were performed in a 10 ml three-neck round bottom glass reactor equipped with a condenser, a temperature well with a thermocouple, and a stir bar. The reactor was placed in a heating mantle on a stir plate and a thermocouple was connected to a temperature controller. The condenser was cooled using an Isotemp 3016D (Fisher Scientific) chiller unit in order to prevent any monomer or solvent evaporation. The nitrogen purge was applied for 20 min before the reaction, and the needle was inserted into the rubber septum, used to cap the condenser, in order to vent the purge. The reactor was then heated (at 5 - 7 °C min^{-1}), and the point when the temperature reached the set point was arbitrarily chosen as t = 0 min. The purge with the reduced flow rate was kept throughout the reaction, and the samples were periodically withdrawn by syringe to track the polymerization progress. Both samples and the crude polymer were precipitated in excess of cold diethyl ether, recovered and vacuum dried at 40 °C overnight.

Synthesis of poly (N-(2-Methacryloyloxyethyl) Pyrrolidone – stat – 9-(4-Vinylbenzyl)-9H-Carbazole) (poly(MAEPYR-stat-VBK)) Statistical Copolymers via NMP.

Table 2-1 lists all the formulations studied. All the copolymerizations were conducted with BlocBuilder and SG1 initiators in DMF (50 wt%) at 90 °C. The molar ratio of SG1 relative to BlocBuilder (r = $[\mathrm{SG1}]_0/[\mathrm{BlocBuilder}]_0$) was 0.1, the VBK initial feed concentration ($f_{VBK,0}$) was varied between 2 - 10 mol%, and the target molecular weight at complete conversion was calculated to be 10, 25 or 50 kg mol^{-1}. The formulation of MV-1, with initial VBK molar composition ($f_{VBK,0}$) 2 mol%, is given as an example (Table 2-1). BlocBuilder (0.048 g, 0.125 mmol), SG1 (0.004 g, 0.012 mmol), MAEPYR (3.01 g, 15.28 mmol), VBK (0.085 g, 0.32 mmol), and DMF (3.10 g, 42.37 mmol) were added to the reactor. The polymerization was performed at 90 °C for 5.3 hours. Samples of 0.1 - 0.15 ml were withdrawn during the reaction to track the polymerization progress, and at the end of the reaction the final yield was 0.99 g (88% conversion; final molar composition of VBK, F_{VBK} = 0.01) with $\overline{M_n}$= 10.2 kg mol^{-1} and $\overline{M_w}$ / $\overline{M_n}$ = 1.58. The procedure for compositional analysis via NMR is shown in the characterization section. The GPC was calibrated using PMMA standards in DMF at 50 °C. The yield was determined gravimetrically and it was lower than expected. This might be due to the choice of the non-solvent used for the precipitation (diethyl ether in this case), since the low molecular weight oligomers that contributed to the overall conversion, as determined by NMR analysis, might have been washed out.

Table 2- 1 Experimental formulations for poly(*N*-(2-methacryloyloxyethyl)-pyrrolidone-*stat*- 9-(4-vinylbenzyl)-9H-carbazole) (poly(MAEPYR-*stat*-VBK)) statistical copolymerizations performed in 50 wt% DMF solution at 90 °C.

ID[a]	Symbol	[BlocBuilder]$_0$ (mol L^{-1})	[SG1]$_0$ (mol L^{-1})	[VBK]$_0$ (mol L^{-1})	[MAEPYR]$_0$ (mol L^{-1})	[DMF]$_0$ (mol L^{-1})	$M_{n,target}$[b] (kg mol^{-1})	$f_{VBK,0}$[c]
MV-1	Δ	0.021	0.002	0.05	2.57	7.12	24.8	0.02
MV-2	○	0.051	0.005	0.10	2.45	7.38	10.0	0.04
MV-3	◊	0.020	0.002	0.10	2.47	7.34	25.2	0.04
MV-4	□	0.011	0.001	0.11	2.55	7.17	49.3	0.04
MV-5	+	0.021	0.002	0.13	2.41	7.48	24.9	0.05
MV-6	*	0.020	0.002	0.20	2.36	7.60	25.8	0.08
MV-7	x	0.020	0.002	0.25	2.21	7.94	24.9	0.10

[a] Experiments for poly(MAEPYR-*stat*-VBK) copolymerizations are denoted MV-Z with M representing *N*-(2-methacryloyloxyethyl)-pyrrolidone, V representing 9-(4-vinylbenzyl)-9H-carbazole, and Z representing the experiment number; [b] The target molecular weight, $M_{n,target}$, was calculated according to $M_{n,target} = M_I + M_m*[m]_0/[I]_0$, where M_I and M_m are the molecular weight of the initiator and monomer, respectively, $[m]_0$ and $[I]_0$ are the initial monomer and initiator concentrations, respectively; [c] $f_{VBK,0}$ is the initial molar fraction of VBK in the feed.

Synthesis of poly (N-(2-Methacryloyloxyethyl) Pyrrolidone – stat – 9-(4-Vinylbenzyl)-9H-Carbazole)-block-poly(N,N-Dimethylacrylamide) (poly(MAEPYR-stat-VBK)-b-poly(DMAA)) Block Copolymers via NMP.

Table 2-2 lists the formulations studied. The general procedure for chain extension experiments was the same as for the copolymerizations. The macroinitiator was synthesized prior to the chain extension experiment, and a fresh batch of DMAA monomer was used. A formulation for chain extension of MV-3 at 110 °C is given as an example below. Macroinitiator MV-3 (0.55 g, 0.04 mmol), DMAA (2.0 g, 20.4 mmol), and DMF (1.9 g, 25.9 mmol) were added to the reactor. For the specific example, polymerization was stopped after 2 hours. Final yield after fractionation was 0.43 g (molar composition of DMAA, $F_{DMAA} = 0.73$) with $\overline{M_n} = 19.9$ kg mol^{-1} and $\overline{M_w}/\overline{M_n} = 2.26$, as measured by GPC relative to PMMA standards in DMF solvent at 50 s^{o}C. Copolymer composition determination by NMR is detailed in the characterization section.

Table 2- 2 Formulations for chain extension experiments using *N,N*-dimethylacrylamide (DMAA) monomer performed in 50 wt% DMF solution at 110 °C and molecular weight characterization for poly(MAEPYR-*stat*-VBK)-*b*-poly(DMAA) block copolymers.

ID[a]	Macroinitiator ID[a]	[Macroinitiator]$_0$ (mol·L^{-1})	[DMAA]$_0$ (mol·L^{-1})	[DMF]$_0$ (mol·L^{-1})	$M_{n,target,2}$[b] (kg mol^{-1})
MV-8	MV-2	0.015	1.7	10.7	11.3
MV-9	MV-3	0.016	5.0	6.3	30.7
MV-10	MV-5	0.009	4.8	6.5	52.3

[a] Experiments for poly(MAEPYR-*stat*-VBK) copolymerizations and chain extensions are denoted MV-Z with M representing *N*-(2-methacryloyloxyethyl)-pyrrolidone, V representing 9-(4-vinylbenzyl)-9H-carbazole, and Z representing the experiment number. [b] The target molecular weight, $M_{n,target,2}$, of the second block was calculated according to $M_{n,target,2} = M_m*[m]_0/[macro]_0$, where M_m is the molecular weight of the monomer, $[m]_0$ and $[macro]_0$ are the initial monomer and macroinitiator concentrations, respectively. The target molecular weight, $M_{n,target,block}$ of the final block can be calculated according to $M_{n,target,block} = M_{n,macro} + M_{n,target,2}$, where $M_{n,macro}$ is the molecular weight of the macroinitiator used.

Synthesis of poly (N-(2-Methacryloyloxyethyl) Pyrrolidone (poly(MAEPYR)) Homopolymer via RAFT Polymerization.

The polymerization was conducted using AIBN as a source of radicals, and CPDTC as a chain transfer agent (CTA) in DMF (50 wt%) at 75°C. The initial ratio of CTA relative to AIBN $[CTA]_0:[AIBN]_0$ was 5. AIBN (0.003 g, 0.019 mmol), CPDTC (0.036 g, 0.104 mmol), MAEPYR (2.53 g, 12.83 mmol), and DMF (2.53 g, 34.61 mmol) were added to the reactor. The polymerization was stopped after 2 hours. The final yield was 0.82 g (88% conversion with $\overline{M_n}$ = 10.9 kg mol^{-1} and $\overline{M_w}/\overline{M_n}$ = 1.60).

2.2.4 Characterization

Polymer Characterization

Gel Permeation Chromatography (GPC)

The number average molecular weight, $\overline{M_n}$, and the dispersity, Đ or $\overline{M_w}/\overline{M_n}$, were determined by gel permeation chromatography (GPC, Water Breeze). GPC was equipped with ultra-violet (UV 2487) and differential refractive index (RI 2414) detectors. The GPC was equipped with 2 ResiPore (3 μm, MULTI pore type, 250 mm x 4.6 mm) columns with a ResiPore guard column (3 μm, 50 mm x 4.6 mm) from Polymer Laboratories. HPLC grade DMF was used as a mobile phase with a flow rate of 0.3 ml min^{-1}. The GPC was calibrated using poly(methyl methacrylate) standards in DMF at 50 °C.

Nuclear Magnetic Resonance Spectroscopy (NMR)

All ^{1}H NMR spectroscopy were performed in $CDCl_3$ using a 400MHz Varian Gemini. Conversion of the MAEPYR was determined by comparing the area associated to the vinyl peaks (Figure 2-1) ($H_{1,2}$ δ = 6.08 and 5.56 ppm) to the area associated to the ethyl spacer hydrogens ($H_{3,4}$ δ = 4.0 for the polymer and δ = 4.25 ppm for the monomer). Conversion of the VBK was determined by comparing the areas associated to the vinyl peaks ($H_{5\text{-}7}$ δ = 6.6, 5.7, and 5.2 ppm) to the area associated to the methylene hydrogens ($H_{8,9}$ δ = 5.5 ppm for the monomer and δ = 5.4 ppm for the polymer). Conversion, X, of the poly(MAEPYR-stat-VBK) copolymerizations was calculated from $X = X_{MAEPYR}\,\omega_{MAEPYR,0} + X_{VBK}\,\omega_{VBK,0}$, where $\omega_{\mathrm{MAEPYR},0}$ and $\omega_{VBK,0}$ are the initial weight fractions of MAEPYR and VBK, respectively.

The final composition of the statistical and/or block copolymers was determined by the ratio of the ethyl spacer protons corresponding to MAEPYR units ($H_{3,4}$, 2H, δ = 4.0), the methylene protons corresponding to VBK units ($H_{8,9}$, 2H, δ = 5.4 ppm), and the methyl protons corresponding to DMAA units ($C\text{-}N(CH_3)_2$, 6H, δ = 3.0 - 3.2 ppm,). For instance, $F_{DMAA} = \frac{I_{DMAA}/6}{I_{MAEPYR}/2 + I_{VBK}/2 + I_{DMAA}/6}$, where I_{DMAA}, I_{MAEPYR}, I_{VBK} are the integrated areas corresponding to DMAA, MAEPYR, VBK polymer peaks, respectively, and F_{DMAA} is the DMAA composition in the final block copolymer.

^{31}P NMR spectroscopy of isolated poly(MAEPYR-stat-VBK) copolymers was recorded in $CDCl_3$ solvent using a 200MHz Varian Gemini. The copolymer was carefully weighed and a known amount of diethyl phosphate (DEP) was added as an internal standard. The ratio of SG1-capped chains to DEP was calculated using the peaks corresponding to SG1 group (δ = 24 - 27 ppm), and DEP (δ = 8 – 9 ppm). This ratio was compared to the molar ratio of copolymer to DEP to obtain the molar percentage of SG1-capped chains in the sample.

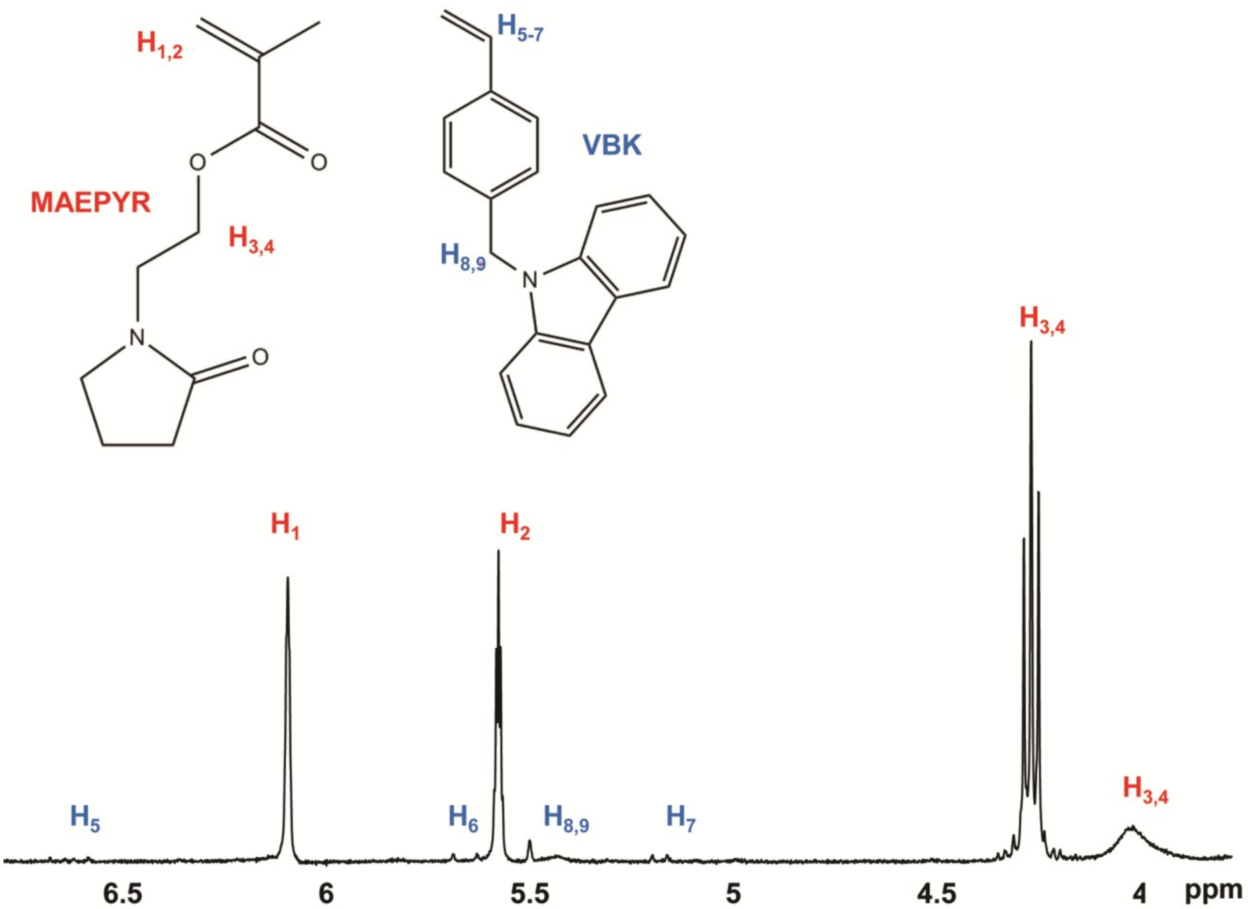

Figure 2- 1 Typical ^1H NMR ($CDCl_3$) spectra of the crude mixture during a poly(MAEPYR-*stat*-VBK) statistical synthesis. The region shown is only where the peaks used for conversion determination occurred. Note that the peak due to the DMF solvent (~ 3 ppm) is not shown in the region of interest. Also, the aromatic protons due to the carbazole ring are at higher chemical shifts.

CPT Measurement

Two techniques were used to report cloud point temperature (CPT) of a polymer in aqueous solution: UV-Vis spectroscopy and dynamic light scattering (DLS).

UV-Vis Spectroscopy

The cloud point temperatures (CPTs) were measured by UV-Vis spectroscopy using a Cary 5000 UV−Vis−NIR spectrometer (Agilent Technologies) equipped with a temperature controlled Peltier thermostatted (6 × 6) multicell holder. The light absorbance was measured at a wavelength of 500 nm. The heating rate and temperature range observed varied from one analysis to another, as these variables were studied. The CPT was determined as the temperature at which the normalized absorbance reached 0.5 on a heating cycle.

Dynamic Light Scattering (DLS)

The Malvern Zetasizer Nano ZS equipped with a 633 nm red laser was used. The samples were filtered using a 0.2 micron filter and then heated in increments of 0.2 °C, allowed to equilibrate for 1 min followed by 10-14 measurements, which were averaged together to give one value at the corresponding temperature. All DLS measurements were performed at a scattering angle (θ) of 173°. For more accurate measurement of the hydrodynamic radius, the refractive index (RI) of a sample has to be estimated. The RI that was used was that of PMMA.

2.3 Results and Discussion

2.3.1 Statistical Copolymer Synthesis

The homopolymerization of methacrylates like MAEPYR using NMP is problematic due to the high equilibrium constant (K) between the dormant and active species, resulting in irreversible termination due to β-hydrogen transfer from the propagating radical to the nitroxide[69]. Recently, NMP of methyl methacrylate (MMA) without any comonomer was successful up until 60% conversion by using a new alkoxyamine based on 2,2-diphenyl-3-phenylimino-2,3-dihydroindol-1-yloxyl (DPAIO) nitroxide[70] with final dispersity close to 1.3 - 1.4. Grubbs and co-workers used *N*-phenylalkoxyamines to homopolymerize MMA up to moderate conversions (up to 50%) while maintaining narrow molecular weight distributions throughout the entire reaction (dispersity of 1.12 - 1.30)[71]. In this study, a commercially available initiator, BlocBuilder, and a controlling comonomer, VBK, are used to yield MAEPYR-rich copolymers. The characteristic plots of the number average molecular weight $\overline{M_n}$ and dispersity $\overline{M_w}/\overline{M_n}$ versus conversion, X, shows a plateau in $\overline{M_n}$ and a significant increase in $\overline{M_w}/\overline{M_n}$ (Figure 2-2).

The first attempt to copolymerize MAEPYR with as little as 2 mol% VBK (MV- 1, Table 2-1) with a target molecular weight at complete conversion of 25 kg mol^{-1} resulted in a relatively fast polymerization, reaching 88% conversion in 5 hours. It followed first-order kinetics in the initial stages (Figure 2-2a) with a noticeable termination at later stages of the polymerization. NMR analysis revealed that at 30 minutes of the reaction, about 80% of VBK monomer (VBK$_m$) was polymerized (Figure 2-3). With almost no controlling comonomer remaining in the mixture, the propagation rates increased drastically and increased the probability of irreversible termination reactions[11]. The number average molecular weight of MV-1 versus conversion is linear in Figure 2-2c. The Đ increased at the early stage of polymerization and then decreased steadily to 1.58 at the final conversion of 88%.

Based on the results presented in Figure 2-2, it showed that the initial concentration of VBK clearly influenced the control of the polymerization. Table 2-1 shows all the formulations studied. Characteristic kinetic plots for poly(MAEPYR-*stat*-VBK) copolymerizations with various VBK compositions are shown in Figure 2-2. The polymerization rate, as indicated by the slope, decreased with increasing VBK initial feed composition. Number average molecular weight ($\overline{M_n}$) increased linearly with conversion up to 60 – 80 % with final copolymers characterized by monomodal molecular weight distributions even though dispersities were somewhat high (Đ < 1.7). The molecular weight data did not follow the theoretical line precisely (Figure 2-2c) for two reasons likely. First, the difference in hydrodynamic volume of the samples and the PMMA standards used for the GPC calibration could be the source for the difference. Second, the deviations from the theoretical line at higher conversions might be due to the presence of irreversible termination reactions. The properties of the final statistical copolymers are listed in Table 2-3. At t = 0 in Figure 2-2, there are conversions 24 % - 38 %, which suggests that fast polymerization occurred during the initial stage. BlocBuilder begins to decompose at much lower temperatures[72] compared to the reaction temperature, and it would initiate the reaction before the set point temperature, which was taken as t = 0. The heating rate was set so that the set point temperature is reached within 10 - 15 minutes so as to minimize the polymerization rate before the prescribed set point was attained. It is interesting to note that in almost all the cases, the controlling comonomer, VBK, was consumed faster than the methacrylate monomer (MAEPYR), which explains the higher VBK content in the final polymer when compared to the initial feed composition. Only for the case of MV-1 is the composition much richer in methacrylate than expected.

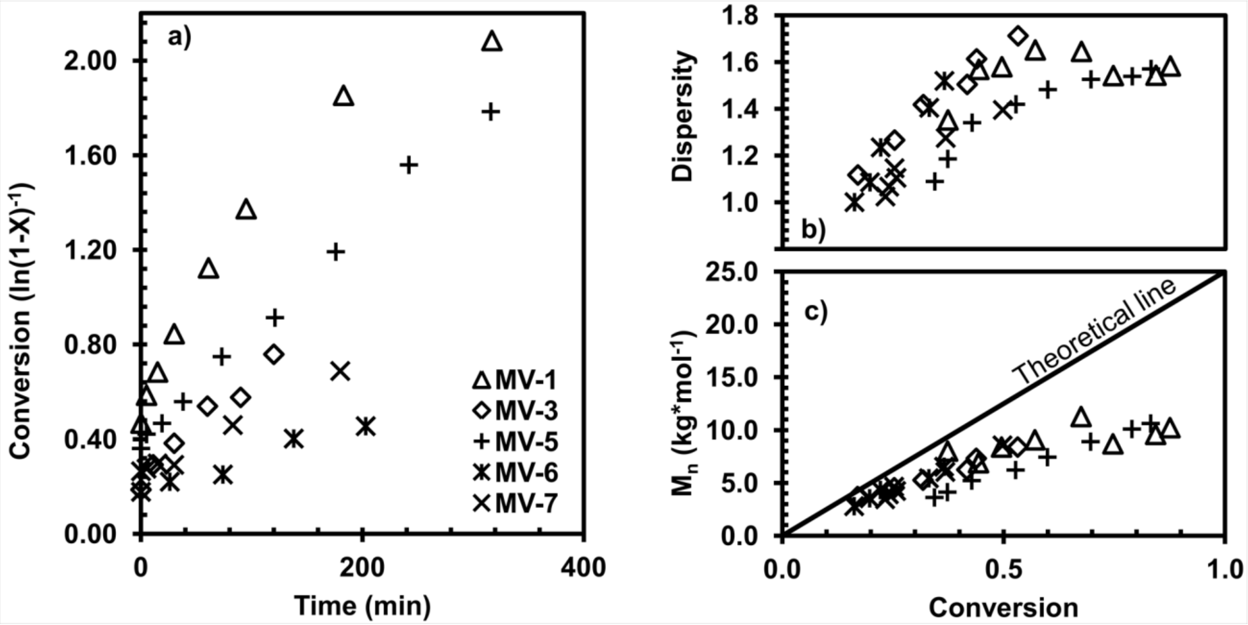

Figure 2- 2 (a) The semi-logarithmic plots of scaled conversion (ln[1-X]$^{-1}$]) (X = conversion) versus time; (b) the dispersity, Đ, versus X plots; (c) the number average molecular weight ($\overline{\boldsymbol{M_n}}$) versus X plots for poly(MAEPYR-*stat*-VBK) copolymerizations at varying VBK feed content, where the symbols are as follows: Δ ($f_{VBK,0}$ = 0.02); ◊ ($f_{VBK,0}$ = 0.04); + ($f_{VBK,0}$ = 0.05); * ($f_{VBK,0}$ = 0.08); x ($f_{VBK,0}$ = 0.10).

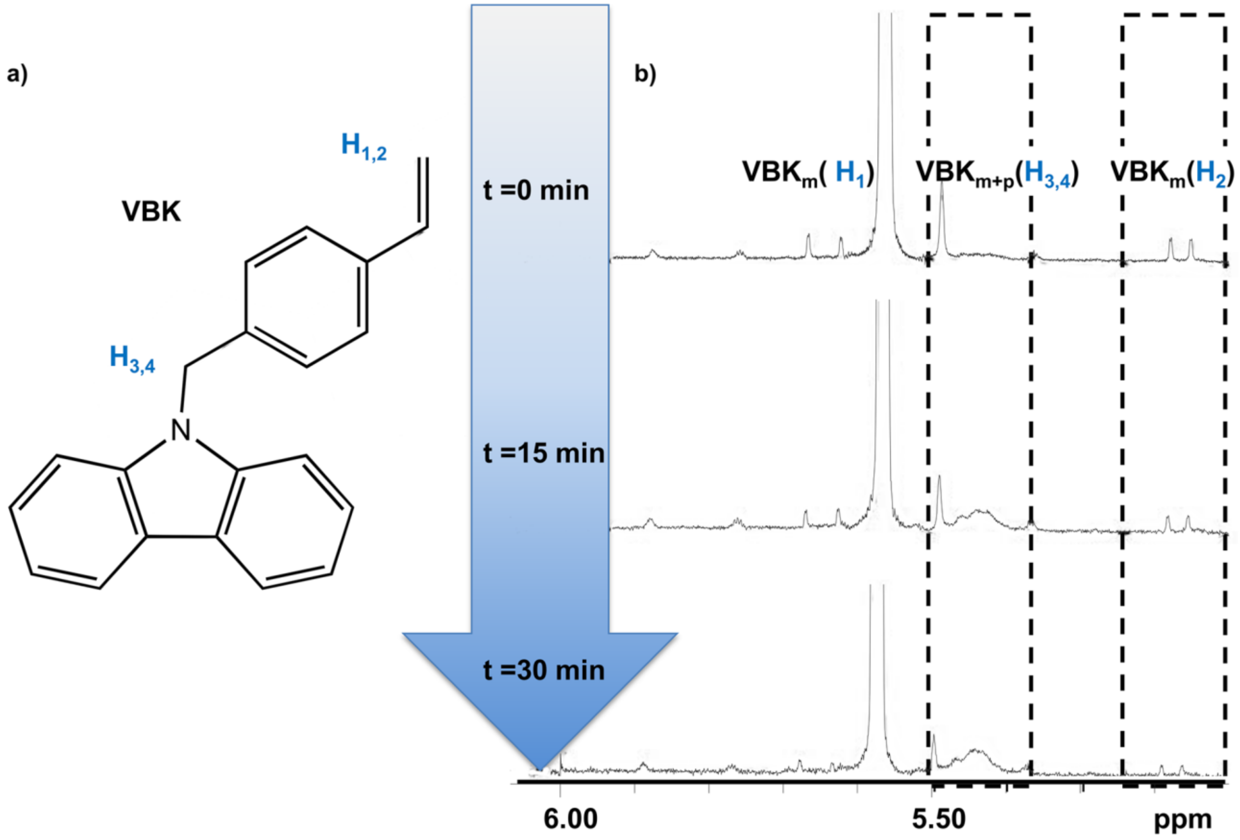

Figure 2- 3 (a) Labeled protons ($H_{1\text{-}4}$) of 9-(4-vinylbenzyl)-9H-carbazole monomer (VBK_m) and the corresponding ^1H NMR spectra are shown in (b) for MV-1 in $CDCl_3$ at various polymerization times. VBK_m are the peaks corresponding to monomer only, and VBK_{m+p} are the peaks corresponding to both monomer and polymer.

Table 2- 3 Molecular weight characterization for poly(MAEPYR-*stat*-VBK) statistical copolymers.

ID[a]	Symbol	$M_{n,target}$ (kg mol^{-1})[b]	$f_{VBK,0}$[c]	F_{VBK}[c]	X[d]	M_n (kg mol^{-1})[e]	M_w/M_n[e]
MV-1	Δ	24.8	0.02	0.01	0.88	10.2	1.58
MV-2	○	10.0	0.04	0.05	0.76	5.9	1.43
MV-3	◊	25.2	0.04	0.06	0.53	8.4	1.71
MV-4	□	49.3	0.04	0.06	0.59	24.1	2.32
MV-5	+	24.9	0.05	0.06	0.83	11.8	1.56
MV-6	*	25.8	0.08	0.16	0.37	8.5	1.59
MV-7	x	24.9	0.10	0.16	0.80	10.3	1.56

[a] Experiments for poly(MAEPYR-*stat*-VBK) copolymerizations are denoted MV-Z with M representing *N*-(2-methacryloyloxyethyl)-pyrrolidone, V representing 9-(4-vinylbenzyl)-9H-carbazole, and Z representing the experiment number; [b] The target molecular weight was calculated according to equation 1; [c] $f_{VBK,0}$ is the initial molar fraction of VBK in the feed; F_{VBK} is the molar fraction of VBK in the final copolymer as determined by ^{1}H NMR spectroscopy; [d] Monomer conversion determined by ^{1}H NMR spectroscopy; [e] Number-average molecular weight ($\overline{M_n}$) and dispersity were determined by GPC.

Figure 2-4 shows the effect of different target molecular weights on the kinetics, while keeping the initial feed composition of the controlling comonomer constant. The theoretical molecular weight depends on the alkoxyamine concentration[11, 73] and can be calculated by Equation 1.

$$M_n = M_I + \frac{[m]_0}{[I]_0} \cdot X \cdot M_m \qquad \text{(Equation 1)}$$

In Equation 1, M_n is the target molecular weight of the final polymer at complete conversion (X = 1); M_I and M_m are the molecular weight of the initiator and monomer, respectively; $[m]_0$ and $[I]_0$ are the initial monomer and initiator concentrations, respectively.

For low target molecular weight, there is sufficiently high alkoxyamine concentration in the solution, and the persistent radical effect (PRE)[11] helps to control the reaction by decreasing the polymerization rate. As the result, the final polymers are characterized by relatively narrow molecular weight distribution (Đ ~ 1.4, Figure 2-4b). In contrast, at low alkoxyamine solution concentration, the PRE is less profound. The polymerization rates are high, and the probability of termination reactions increases, which is exemplified by a broad molecular weight distribution

(Đ ~ 2.5, Figure 2-4b). Number average molecular weights for all three experiments in Figure 2-4 increased linearly with conversion up to approximately 60% conversion.

A typical set of GPC chromatograms for the poly(MAEPYR-*stat*-VBK) statistical copolymerizations is shown in Figure 2-5a, whereas Figure 2-5b shows GPC traces for chain extension experiments with DMAA. The growth of the chains with time in both cases is indicated by the shift of the peaks in the chromatogram to lower elution times (higher molecular weight). The tailing on the low molecular weight side is likely due to irreversible termination.

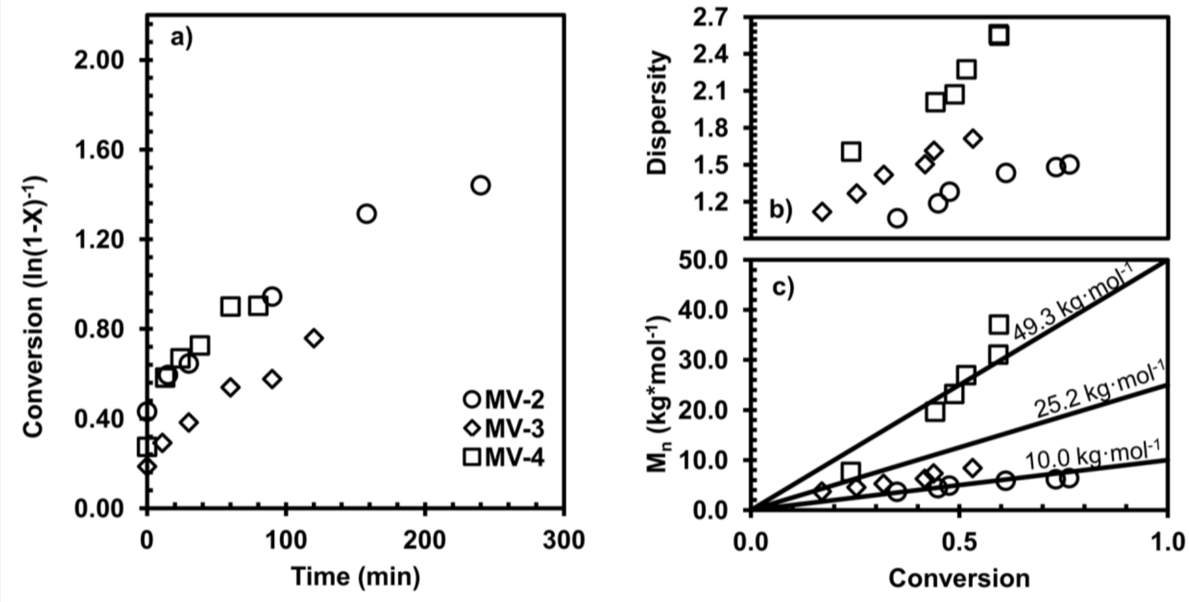

Figure 2- 4 (a) The semi-logarithmic plots of scaled conversion (ln[1-X]$^{-1}$]) (X = conversion) versus time; (b) the dispersity, Đ, versus X plots, and (c) the number average molecular weight ($\overline{M_n}$) versus X plots for poly(MAEPYR-stat-VBK) copolymerizations at varying target molecular weight, where ○ ($M_{n,target}$ = 10.0 kg mol^{-1}); ◊ ($M_{n,target}$ = 25.2 kg mol^{-1}); □ ($M_{n,target}$ = 49.3 kg mol^{-1}).

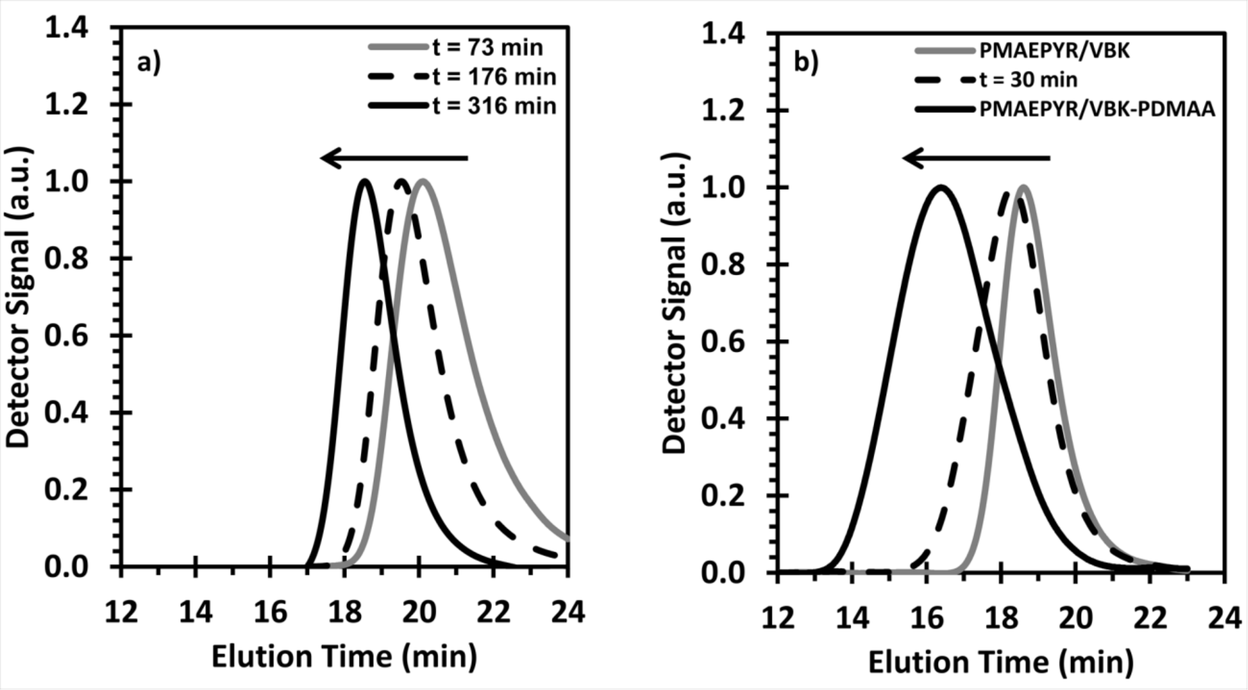

Figure 2- 5 Gel permeation chromatograms (GPC) of (a) a characteristic copolymerization of MV-5; (b) DMAA chain extension (MV-10) done in a 50 wt% solution in DMF at 110°C from MV- 5 macroinitiator.

2.3.2 Block Copolymer Synthesis

To test the ability of the final polymers to reinitiate a fresh batch of monomer, chain extension experiments were performed with DMAA monomer in DMF solvent (Scheme 2-1). The formulations for all the chain extension experiments are listed in Table 2-2. The monomodal shift in the GPC chromatograms (Figure 2-5b) for MV-10 suggests that the macroinitiator (MV-5) was significantly SG1-terminated. Similar behavior was observed for the other two chain extension experiments (MV-8 and MV-9). Table 2-4 lists the properties of all final block copolymers. The dispersity values of the final chain-extended samples are quite high, which is suggestive of poor re-initiation. Fractionation was attempted to separate the dead chains from the block copolymer, but with little success; however, the DMAA content in the final polymer decreased slightly (for instance, $F_{DMAA} = 0.73$ for MV-9 after the fractionation and 0.90 before the fractionation). ^{31}P NMR spectroscopy was used to determine the amount of SG1 present at the chain ends (since phosphorus is present in SG1[72]). For instance, it was found that MV-2 was

13 % living. Such a low fraction of SG1-terminated chains explained the poor re-initiation and broad dispersities of the final block copolymers. However, ^{31}P NMR spectroscopy might be misleading since the concentration of phosphorus in the polymer was very low and could lead to substantial error.[63, 74] The GPC chromatograms of the chain extensions shown in Figure 2-5 did not indicate an obvious peak corresponding to unreacted macroinitiator; this may be due to the molecular weights/hydrodynamic volumes of the species not being very different from one another.

Table 2- 4 Molecular weight characterization for poly(MAEPYR-*stat*-VBK)-*b*-poly(DMAA) block copolymers.

ID^a	Macroinitiator ID^a	Macroinitiator M_n^{b} (kg mol^{-1})	Macroinitiator M_w/M_n^{b}	M_n^{b} (kg mol^{-1})	M_w/M_n^{b}	F_{DMAA}^{c}
MV-8	MV-2	5.9	1.43	12.4	2.37	0.92
MV-9	MV-3	8.4	1.71	19.9	2.26	0.73
MV-10	MV-5	11.8	1.56	53.5	2.96	0.89

[a] Experiments for poly(MAEPYR-stat-VBK) copolymerizations and chain extensions are denoted MV-Z with M representing *N*-(2-methacryloyloxyethyl)-pyrrolidone, V representing 9-(4-vinylbenzyl)-9H-carbazole, and Z representing the experiment number; [b] Number-average molecular weight ($\overline{M_n}$) and dispersity index were determined by GPC; [c] F_{DMAA} is the molar fraction of DMAA in the final block copolymer as determined by ^{1}H NMR spectroscopy.

2.3.3 Solution Properties of Statistical and Block Copolymers

The MAEPYR-rich statistical copolymers and block copolymers were tested for thermo-responsive behaviour in aqueous media. Properties of stimuli-responsive polymers are connected to the microstructure of the polymer; therefore, well-defined polymers with narrow molecular weight distributions are essential for clear determination of CPT.[39, 47-49] Davis and co-workers synthesized MAEPYR homopolymers via conventional polymerization.[61] Although there is no information given about the microstructure of the resulting polymers, the CPTs in water (0.7 wt%) were measured at a heating rate of 1°C min^{-1} and the CPTs ranged between 29 - 34 °C[61]. Cai et al. reported CPTs of 2 wt% solutions ranging from 52.8 - 71.5 °C for MAEPYR homopolymers synthesized by RAFT polymerization with weight-average molecular weights of 105.4 to 20.6 kg mol^{-1}, respectively[60]. Here, the effect of composition, solution concentration and heating rate on CPT was studied.

Effect of Composition on the Transition of Statistical Copolymers.

Poly(MAEPYR-*stat*-VBK) statistical copolymers exhibited tuneable cloud point temperature (CPT) by varying VBK content. Increasing the content of the more hydrophobic monomer, VBK, in the final copolymer structure will decrease the CPT due to the decreased degree of hydrogen bonding with water.[30, 75, 76] Poly(MAEPYR) homopolymer (see experimental section for details about the synthesis and characterization) has a CPT of 59.0 °C ($\overline{M_n}$= 10.9 kg mol^{-1}), and the CPT decreased to 49.7 °C (for MV-1 with F_{VBK} = 1 mol%, $\overline{M_n}$ = 10.2 kg mol^{-1}) and 39.6 °C (for MV-5 with F_{VBK} = 6 mol%, $\overline{M_n}$ = 11.8 kg mol^{-1}) for poly(MAEPYR-*stat*-VBK) statistical copolymers at 1 wt% solution concentration. Poly(MAEPYR) homopolymer ($\overline{M_n}$= 10.9 kg mol^{-1}) has a CPT of 53.5 °C at 2 wt%, which is slightly different from the values reported by Cai (71.5 °C at 20.6 kg mol^{-1}) at the same concentration. The difference may arise from different polymer samples used (e.g. molecular weight is relative to either PMMA or PS standards, for this and Cai's work, respectively), due to higher dispersity values associated with polymers used in this work (compared to Đ of 1.11-1.13 for polymers used in Cai's work) and/or due to the conditions used for the CPT determination (e.g. heating rates, and turbidity versus light scattering methods).

Effect of Solution Concentration on the Transition of Statistical Copolymers.

Particle size was measured by dynamic light scattering (DLS, see the experimental section) for the statistical copolymers during the phase transition. poly(MAEPYR-*stat*-VBK) statistical copolymers with low VBK content (e.g. MV-1) were readily soluble at room temperature in deionized water. The light scattering intensity was low, as measured by DLS, from room temperature until about 39 °C (Figure 2-6a). During heating, the intensity increased significantly when the temperature reached the critical temperature, which is the CPT.[40] From Figure 2-6a it is seen that the intensity increased dramatically at 42 °C. The intensity is related to the particle size: larger particles scatter light more, which would result in higher intensity[77]. Hence, it is possible to determine the CPT by monitoring the change in the population of particle sizes. Figures 2-6c and 2-6b show the temperature dependence of average hydrodynamic radius, <R_h>, of poly(MAEPYR-*stat*-VBK) chains (MV-1, $\overline{M_n}$= 10.2 kg mol^{-1}, F_{VBK} = 0.01) in one heating cycle as measured by DLS, and normalized absorbance of the heating ramp of the same sample as measured by UV-Vis spectroscopy, respectively. The CPT at 50 % normalized absorbance is 49.7 ^{o}C and 40.9 ^{o}C for 0.5 and 1 wt% solutions, respectively, and the $<R_h>$ increased at a temperature above 47 and 42 °C, respectively. The $<R_h>$ measurements showed considerable scatter above the CPT, which is likely due to sedimentation.[60] The CPT by DLS was determined when the intensity-weighted particle distribution was shifted from the lower to the higher $<R_h>$ as indicated in Figure 2-6a. The transparent solution became opaque when the temperature was above the CPT due to aggregation[40, 78] of polymer chains. The temperature-induced phase separation was reversible, and the polymer solution became clear again when the temperature was below the CPT.

At lower solution concentration (Figure 2-7) the CPT increases since the formation of polymer aggregates is a much slower process at low polymer concentrations[78]. Depending on the solution concentration, MV-1 exhibited a difference of as much as 16.6 °C in CPTs (from 50.9 °C for 0.3 wt% solution to 34.3 °C for 4 wt% solution). These observations are consistent with literature.[24, 78-81] For instance, the CPT for poly(DMAEMA-*stat*-styrene) copolymers decreased by 7 - 10 °C when the solution concentration increased from 0.1 to 0.3 wt%.[79] Similarly, PNIPAM polymer samples showed a significant concentration dependence below 5 wt%, and the curve reaches a plateau at higher concentrations (15-20 wt%).[78] The polymer samples, other than MV-1 and MV-5, were water-insoluble, and were not considered for the analysis.

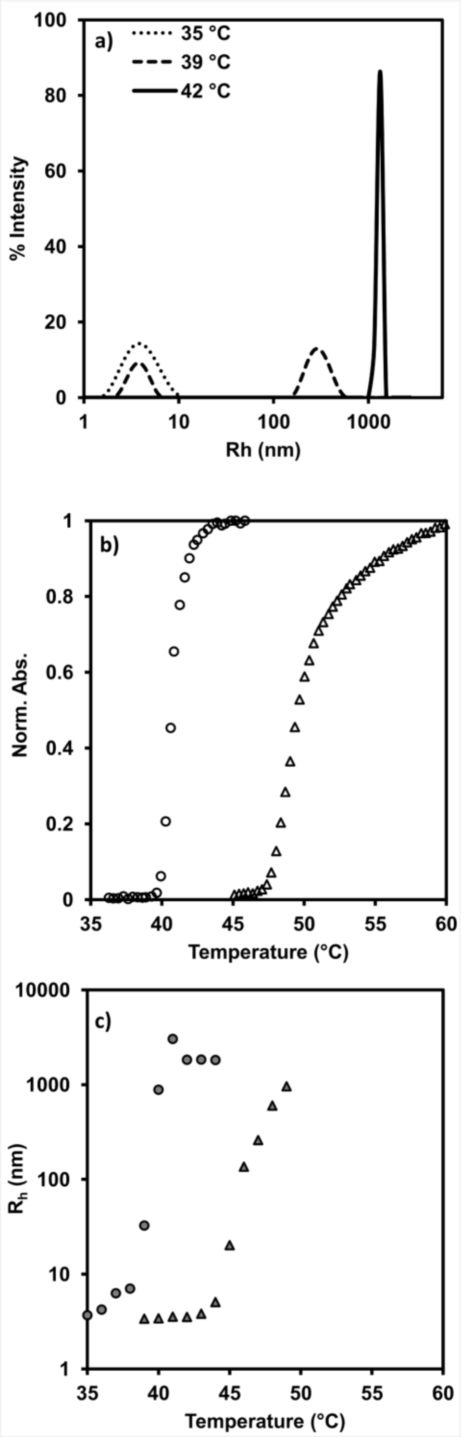

Figure 2- 6 (a) The distribution of different particle size populations during DLS measurement of statistical poly(MAEPYR-*stat*-VBK) copolymer MV-1 ($\overline{M_n}$ = 10.2 kg mol^{-1}, Đ = 1.58, F_{VBK} = 0.01) at 1 wt% solution during a heating ramp; (b) The normalized absorbance as measured by UV-Vis and (c) average hydrodynamic radius (<R_h>) as measured by DLS of MV- 1 at 0.5 wt% solution (triangles) and 1 wt% solution (circles) during one heat cycle.

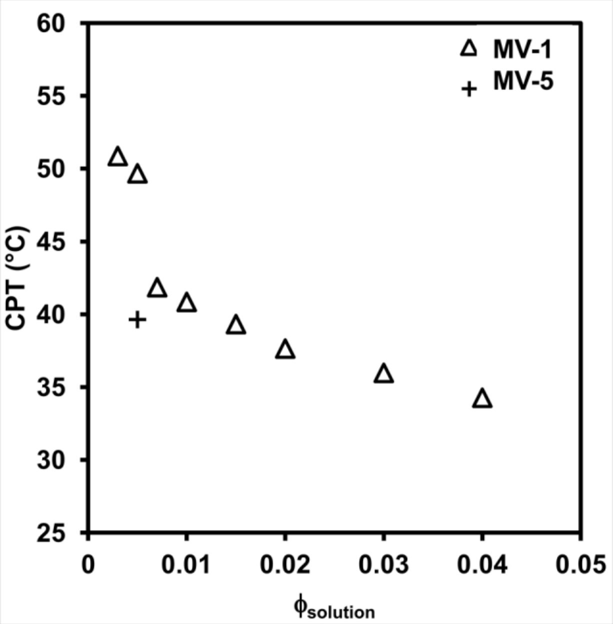

Figure 2- 7 CPT dependence of MV-1 (Δ, $\overline{M_n}$ = 10.2 kg mol^{-1}, Đ = 1.58, F_{VBK} = 0.01) and MV-5 (+, $\overline{M_n}$ = 11.8 kg mol^{-1}, Đ = 1.56, F_{VBK} = 0.06) samples on composition and MV-1 samples on solution concentration as measured by UV-Vis spectroscopy with a heating ramp of 1 °C min^{-1}.

Hysteresis and Effect of Scanning Rate on the Transition of Statistical Copolymers.

One of the most important properties of "smart" polymers is the reversibility of the phase transition. It was found that the temperature-induced phase separation was reversible, but the hysteresis effect was noticeable since the temperature of the phase transition in the cooling process was different from the one in the heating process. The hysteresis observed was as low as 2 °C and as high as 10 °C when the rate of heating and cooling was 1 °C min^{-1}. Cai et al. reported no profound hysteresis effect for one heating-cooling cycle for one of the many poly(MAEPYR) homopolymers they examined ($\overline{M_w}$ = 105.4 kg mol^{-1})[60]. In our study, the $\overline{M_n}$s of the copolymers studied were 10.2-11.8 kg mol^{-1} (relative to PMMA standards) and the hysteresis effect becomes larger as the molecular weight decreases: smaller chains tend to form larger aggregates due to interchain association, which are more difficult to dissociate during the cooling cycle due to the increased degree of hydrogen bonding.[23, 81] It is interesting to note that the poly(MAEPYR) homopolymer (synthesized by RAFT for comparison, see experimental section) exhibited very little hysteresis of 2 °C when observed under the same conditions (1 wt%

solution, heating/cooling rate of 1 °C min^{-1}) as MV-1 copolymer. The observed difference for our samples suggests the presence of weak van der Waals interactions[39] and/or hydrophobic interactions of the polymer's backbone with the ethyl spacers and the carbazole groups from the VBK comonomer.

The CPT strongly depends on the heating rate[76, 78, 82]. As the heating rate was increased, the CPT for MV-1 samples at 1 wt% concentration was found to increase as well. For example, the CPT increased from 39.8 °C to 45.2 °C for the heating rates ranging from 0.2 to 4 °C min^{-1}, respectively. Similar behavior was observed previously in other systems.[24, 78, 82] For instance, increasing the heating rate from 0.02 to 5 °C min^{-1} resulted in about 11 °C increase in CPT for PNIPAM, as determined by turbidity methods.[78] Poly(*N*,*N*-diethylacrylamide) (DEAAM) showed only a 6 °C increase in CPT when the heating rate was altered from 0.06 to 5°C min^{-1}.[82] Polymer-polymer interactions responsible for the phase separation are time-dependent and at higher heating/cooling rates there is less time to react to the environmental change.[76, 82] As a result, the transitions become more diffusive[24, 82], with a partial loss of reversibility[24]. For very high heating rates (3 - 4 °C min^{-1}), the transition of MV-1 samples during the cooling process was very broad, and the solution became clear only at room temperature.

Transition of Block Copolymers.

For the poly(MAEPYR-*stat*-VBK) statistical copolymers, CPT was tuned by the inclusion of the more hydrophobic monomer, VBK, which resulted in lower CPTs as VBK content increased. It is possible to tune CPT in the opposite direction by chain-extending the copolymer with a hydrophilic monomer. Many water-soluble monomers are polymerizable by NMP, including *N*,*N*-dimethylacrylamide (DMAA)[83], *N*-vinylpyrrolidone (VP)[43], 2-*N*-morpholinoethyl acrylate (MEA)[24] and 4-acryloylmorpholine (4AM)[84]. In this study, DMAA was used in the synthesis of a hydrophilic block. With the temperature changes, the block copolymer might gain or lose its amphiphilicity, resulting in formation or dissolution of micelles.[30] There are two types of micelles that can be formed. One type consists of the temperature responsive corona, and the other one has the temperature responsive inner core. In the case of poly(MAEPYR-*stat*-VBK)-*b*-poly(DMAA) block copolymers, the hydrophilic DMAA block would form the outer shell, and the inner core would consist of the temperature responsive copolymer resulting in stable micelle formation below the LCST.[64] Figure 2-8 shows the temperature dependence of average hydrodynamic radius, <R_h>, of poly(MAEPYR-*stat*-VBK)-*b*-poly(DMAA) chains (MV-8 and MV-9) in one heating cycle as measured by DLS, and normalized absorbance on the heating ramp of the same sample as measured by UV-Vis spectroscopy. The increase of average size near the CPT suggests the presence of intermicellar aggregation[85], which is minimal due to the hydrophilic poly(DMAA) block. As a result, the final average hydrodynamic radius for the block copolymer is smaller than that of the statistical copolymers.[64] Also, above the LCST, the hydrophobic effect in the core might disappear due to the interactions of the hydrophilic block, if it is too long, resulting in micelle destruction.[30] Addition of the hydrophilic poly(DMAA) block slowed the rate of phase transition for the block copolymers, compared to the statistical copolymers. From Figure 2-8 it is seen that the phase transition observed by UV-Vis spectroscopy occurs over several tens of degrees (45 - 85 °C for MV-8 chains, for example). Similar behavior was observed in the literature.[64, 85] Dispersity of the final polymer influenced the phase transition as well. Smaller chains tend to form larger aggregates due to additional hydrogen bonding present in the interchain associations, whereas larger chains are likely to undergo only intrachain contractions.[23] The two types of interactions do not occur simultaneously. With the broad molecular weight distributions (for example, Đ = 2.26 - 2.96 for MV-8, MV-9, MV-10 polymers) the transition will become more diffuse as a result of the difference in time required to form aggregates for chains of different length.

As predicted, the hydrophilic monomer shifted the CPT upwards, if compared to the CPT of the precursor MV-1. The CPTs of the macroinitiators (MV-2 and MV-3 in this case) were not determined due to limited solubility of the polymer in aqueous solution. The final CPTs for block copolymers as determined by UV-Vis spectroscopy and DLS are summarized in Table 2-5. There is a discrepancy between the determined CPT values, which is solely due to the analytical technique used. UV-Vis spectroscopy relies on turbidity measurements, so it is sensitive only to the macroscopic phase separation, which is a slow process at low solution concentration.[78] DLS, on the other hand, can detect the collapse of a single polymer chain[78], before the macroscopic phase separation, which occurs usually at a higher temperature. From Figure 2-8 it is seen that the transition, as determined by DLS, is sharper than the one determined by UV-Vis; therefore, CPT values for block copolymers were reported from the DLS measurements.

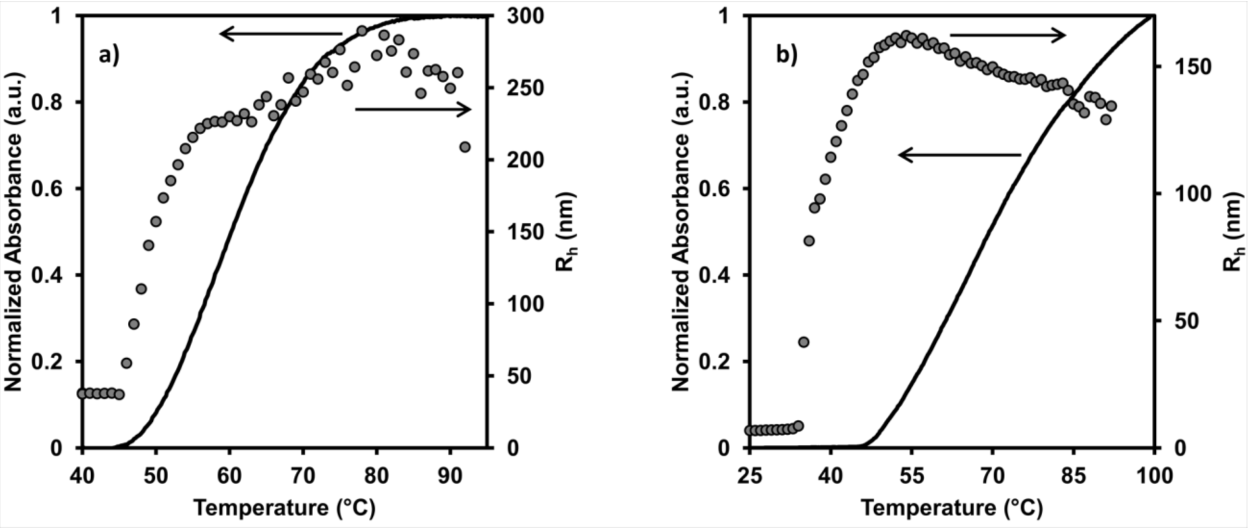

Figure 2- 8 Temperature dependence of the normalized absorbance (black line) as measured by UV-Vis during the heat cycle and average hydrodynamic radius (<R_h>) (grey circles) as measured by DLS during the heat cycle of (a) MV-8 chains ($\overline{M_n}$= 12.4 kg mol^{-1}, Đ = 2.37, F_{DMAA} = 0.92); (b) MV-9 ($\overline{M_n}$ = 19.9 kg mol^{-1}, Đ = 2.26, F_{DMAA} = 0.73), both in 1 wt% solution.

Table 2- 5 The difference in the CPTs for poly(MAEPYR-*stat*-VBK)-*b*-poly(DMAA) block copolymers as determined by UV-Vis spectroscopy and DLS, and the corresponding CPT values determined on a heating ramp.

ID[a]	Macroinitiator ID[a]	CPT by UV-Vis (°C)	CPT by DLS (°C)	$\phi_{solution}$ (wt%)
MV-8	MV-2	60.3	50	1
MV-9	MV-3	69.4	39	1
MV-10	MV-5	82.9	48	1
MV-10	MV-5	66.2	n/a	2

a) Experiments for poly(MAEPYR-stat-VBK) copolymerizations and chain extensions are denoted MV-Z with M representing *N*-(2-methacryloyloxyethyl)-pyrrolidone (MAEPYR), V representing 9-(4-vinylbenzyl)-9H-carbazole (VBK), and Z representing the experiment number. Composition and molecular weight data of the final blocks can be found in Table 2-4.

Stability of Statistical and Block Copolymers.

The stability of the phase transition was tested by observing the changes in particle size over a prolonged period of time. The 1 wt% solutions of statistical and block copolymers, MV-1 and MV-10, respectively, were held above the CPT at 50 °C for 15 hours (Figure 2-9). The changes in <R_h> for MV-1 over the 15-hour period indicated that the system was not stable. At the end of the experiment, the polymer settled at the bottom of the vial, which suggested that macrophase separation had occurred[39]. In contrast, the changes in <R_h> are less profound for MV-10, indicating that the micelles formed were relatively stable.

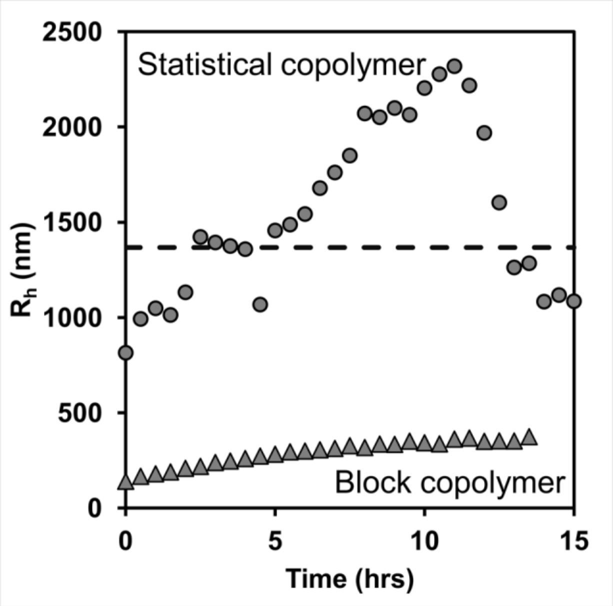

Figure 2- 9 Time dependence of the average hydrodynamic radius (<R_h>) of 1 wt% statistical copolymer (MV-1, $\overline{M_n}$ = 10.2 kg mol^{-1}, Đ = 1.58) and block copolymer (MV-10, $\overline{M_n}$ = 53.5 kg mol^{-1}, Đ = 2.96) solutions at a constant temperature of 50 °C.

2.4 Conclusion

The BlocBuilder/SG1 initiators were able to copolymerize MAEPYR-rich compositions in a relatively controlled manner with a minimum of 5 mol% VBK in the initial feed to give linear number average molecular weight $\overline{M}_n$ versus conversion (until about 60% conversion) with fairly narrow molecular weight distributions of the final polymers (dispersity of 1.4 - 1.7). The ability of the final copolymers to reinitiate a fresh monomer batch was tested using DMAA monomer. In all cases studied, the growth of the polymer chains was monitored via GPC, where a shift of the peak to a lower elution time indicated the increase in molecular weight. The final statistical and block copolymers were tested for LCST-type behavior in aqueous solutions. The effect of VBK composition shifted the CPT from 49.7 °C (for MV-1 with $\overline{M_n}$ = 10.2 kg mol^{-1} and F_{VBK} = 0.01) to 39.6 °C (for MV-5 with $\overline{M_n}$ = 11.8 kg mol^{-1} and F_{VBK} = 0.06) at 1 wt% solution concentration. The CPT also decreased with increasing solution concentration, and MV-1 exhibited a difference of as much as 16.6 °C in CPTs (from 50.9 °C for 0.3 wt% solution to 34.3 °C for 4 wt% solution). The CPT was found to be a function of the heating/cooling rate, and the transitions became more diffusive in nature at higher rates. For the block copolymers, the particle size measurements indicated the block copolymers had a broader transition compared to statistical copolymers and that the block copolymer micelles were relatively stable upon prolonged heating above the CPT.

2.5 Connection Between Manuscripts

The kinetic study of MAEPYR/VBK statistical copolymers by NMP (Chapter 2) led to the conclusion that it was possible to control the polymerization of methacrylate with the addition of 5 mol% of the controlling comonomer to construct copolymers with reasonably narrow molecular weight distributions. Tailored polymer structures are essential for various applications, and polymers with pyrrolidone functionalities show promise in the biomedical field due to their desired properties, such as water solubility, biocompatibility and coordination capacity.[39] The subsequent study of the solution properties of the resulting copolymers revealed that the CPT can be monitored by the copolymer composition, the solution concentration and heating rate. The following step was to investigate polymerization of another family of nitrogen-containing temperature-responsive polymers, polyacrylamides, by CRP methods. The acrylamide monomer with secondary amine functionality, *N*-(3-methoxypropyl) acrylamide (MPAM), has not been polymerized by CRP methods previously, and the conflicting reports in literature regarding its solution properties with temperature changes urge us to apply CRP methods for controlled synthesis and hopefully unambiguous determination of CPT (Chapter 3).

3. Using Controlled Radical Polymerization To Confirm The Lower Critical Solution Temperature Of A *N*-(Alkoxyalkyl) Acrylamide Polymers In Aqueous Solution.

N-(3-methoxypropyl) acrylamide (MPAM) was polymerized by controlled radical polymerization (CRP) methods such as nitroxide-mediated polymerization (NMP) and reversible addition fragmentation chain-transfer polymerization (RAFT). Previous MPAM conventional radical polymerizations yielded homopolymers with conflicting reports about lower critical solution temperature (LCST) behavior in aqueous solutions. CRP was expected to yield well-defined polymers with sharp LCST transitions. NMP with the BlocBuilder (2-([*tert*-butyl[1-(diethoxyphosphoryl)-2,2-dimethylpropyl]amino]oxy)-2-methylpropanoic acid) and SG1 ([*tert*-butyl[1-(diethoxyphosphoryl)-2,2-dimethylpropyl]amino]oxidanyl) initiating system revealed low yields and lack of control (high dispersity, Đ ~ 1.5 - 1.6, and inhibition of chain growth). However, RAFT was far more effective, with linear number average molecular weight, $\overline{M_n}$, versus conversion, X, plots, low Đ ~ 1.17 - 1.47 and the ability to form block copolymers using *N*,*N*-diethylacrylamide (DEAAM) as the second monomer. Poly(MPAM) (with $\overline{M_n}$ = 14.3 - 25.2 kg mol^{-1}) thermoresponsive behaviour in aqueous media revealed LCSTs between 73 and 92 °C depending on solution concentration (ranging from 1 to 3 wt%). The molecular weight and the molecular weight distribution were the key factors determining the cloud point temperature (CPT) and the sharpness of the response, respectively. Poly(MPAM)-*b*-poly(DEAAM) block copolymer ($\overline{M_n}$= 22.3 kg mol^{-1}, Đ = 1.41, molar composition F_{DEAAM} = 0.38) revealed dual LCSTs with both segments revealing distinctive CPTs (at 75 °C and 37 °C for poly(MPAM) and poly(DEAAM) blocks, respectively) by both UV-Vis and dynamic light scattering (DLS).

3.1 Manuscript Introduction

Thermo-responsive polymers, with temperature being the trigger, undergo a thermally induced phase separation such as a lower critical solution temperature (LCST) in solution. *N*-substituted poly(acrylamide)s, such as poly(*N*,*N*-ethylmethylacrylamide), poly(*N*,*N*-diethylacrylamide), poly(*N*-isopropylacrylamide), poly(*N*-*n*-propylacrylamide), are one such representative group of temperature responsive polymers exhibiting this behavior.[30, 86-88] Poly(*N*-alkoxyacrylamide)s, such as poly(*N*-2-ethoxyethylacrylamide), poly(*N*-3-ethoxypropylacrylamide), are another family of temperature-responsive polymers, and the polymer's LCST can be fine-tuned even further, if compared to poly(alkylacrylamides), due to the presence of ether groups.[89] Acrylamide-based polymers with thermoresponsive behavior can be applied in different fields, including but not limited to biomedical research (e.g. for vascular embolization[90], liposome modification for drug delivery[91, 92]), material coatings[93], enhanced oil recovery[94], inhibitors for hydrate formation[95], and thickeners in cosmetics[96].

The properties of the polymer, such as the molecular weight distribution, have an impact on the thermal responsiveness. Controlled polymerization method has allowed clearer determination of LCST behaviour of many polymers due to its ability to reduce the dispersity when compared to conventional radical polymerization. For example, pyrrolidone-based polymers had no LCST or broad LCST transitions when using conventional radical polymerization.[61] Later work with controlled radical polymerization (CRP) techniques showed a clear LCST at 52.8 – 71.5 °C[39, 60] for *N*-(2-methacryloyloxyethyl)-pyrrolidone (MAEPYR) homopolymers and 34.3 – 50.9 °C[97] for its statistical copolymers with 9-(4-vinylbenzyl)-9H-carbazole (VBK). Well-defined molecular weight and narrow molecular weight distribution are essential for precise LCST transitions, which are usually inferred from the cloud point temperature (CPT).[87] CRP techniques allow precise control over the microstructure and the molecular weight distribution, just like truly living polymerizations. Unlike traditional ionic polymerization for instance, CRP does not require stringent reaction conditions, while providing a similar level of control over the molecular weight and chain end functionality. The most popular CRP techniques are nitroxide-mediated polymerization (NMP)[42, 55-57], atom transfer radical polymerization (ATRP)[58, 59] and reversible addition−fragmentation chain transfer (RAFT)[51-54]. There is less post-reaction processing and manipulations for NMP, unlike ATRP and RAFT, where the metal catalyst (ATRP) or odorous sulphur-based chain transfer agent

(RAFT) often have to be removed. Nonetheless, both RAFT and ATRP methods have been applied successfully in bio-applications.[98, 99] NMP generally has been limited to the kinds of monomer it can polymerize (namely styrenics), whereas both RAFT and ATRP have good tolerance towards functional groups of various monomers[87]. However, recent research suggests NMP is viable towards functional monomers like acrylamides.[100-102]

NMP of *N*,*N*-substituted acrylamides yielded different levels of control depending on the number of substituents. The acrylamide with a primary amine group, *N*-acrylamide (AM), was polymerized in aqueous solution using SG1 nitroxide ([*tert*-butyl[1-(diethoxyphosphoryl)-2,2-dimethylpropyl]amino]oxidanyl) and Vazo56 initiator (2,2-azobis(2-methylpropionamidine) dihydrochloride).[100, 103] The final dispersities for all studied conditions was between 1.06 - 1.37, depending on whether conventional heating or a microwave irradiation method was used.[103] Zetterlund studied NMP of *N*-isopropylacrylamide (NIPAM), an acrylamide with a secondary amine group, using SG1 nitroxide in either supercritical carbon dioxide or organic solvent.[104, 105] It was found that chain transfer to solvent limited the polymerization.[105] The acrylamide with a tertiary amine group, 4-acryloylmorpholine (4AM), has been polymerized in a controlled manner by NMP recently by our group[84] and by Schubert et al.[106] using the unimolecular alkoxyamine BlocBuilder (2-([*tert*-butyl[1-(diethoxyphosphoryl)-2,2-dimethylpropyl]amino]oxy)-2-methylpropanoic acid). The 4AM homopolymerizations were well-controlled (Đ < 1.4) over a wide range of temperatures.[84]

The controlled homopolymerization of acrylamides, such as NIPAM, is possible by RAFT using AIBN initiator (2,2'-azobisisobutyronitrile) and DMP (2-dodecylsulfanylthiocarconylsulfanyl-2-methylpropionic acid) chain transfer agent (CTA).[87] Different levels of control were achieved for acrylamides with secondary amine functionality (or mono-*N*-substituted acrylamides) and for acrylamides with tertiary amine functionality (or di-*N*-substituted acrylamides). It was found that di-*N*-substituted acrylamides can be better controlled by RAFT than mono-*N*-substituted acrylamides due to higher reactivity of the monomers and due to formation of more stable radicals.[87] For the di-*N*-substituted acrylamides the dispersities were lower (Đ < 1.2 versus Đ > 1.3), polymerization rates were faster and there was less negative deviation from the theoretically expected molecular weight.[87] McCormick and co-workers reported RAFT polymerization of various other acrylamide monomers using different CTAs.[107]

In this work, we attempted to synthesize *N*-(3-methoxypropyl) acrylamide (MPAM) homopolymers by CRP techniques, mainly NMP and RAFT. MPAM has been polymerized by conventional free radical polymerization[108, 109], and to the best of our knowledge, MPAM homopolymerization by CRP methods has not been reported. Firstly, NMP of MPAM with BlocBuilder and SG1 initiators was attempted (Scheme 3-1a). Further, RAFT via AIBN/DMP was applied towards MPAM homopolymerization (Scheme 3-1b). These results will highlight the possibilities of BlocBuilder-mediated NMP and/or RAFT to synthesize acrylamide homopolymers with secondary amine functional group and with more sophisticated microstructures tailored for thermoresponsive materials. Following the study of the polymerization techniques, the thermo-responsive behaviour of poly(MPAM) homopolymers and block copolymers in aqueous solution was investigated in more detail since reports of the LCST of poly(MPAM) were inconclusive. Ito[109] reported a cloud point of 44.5 °C for poly(MPAM) in 1 % solution, whereas Yamazaki et al.[108] found no phase transition for 2 kg mol^{-1} samples at 0.5 wt% and even higher molecular weight samples at 0.1 wt% when the solution was heated up to 60 °C.

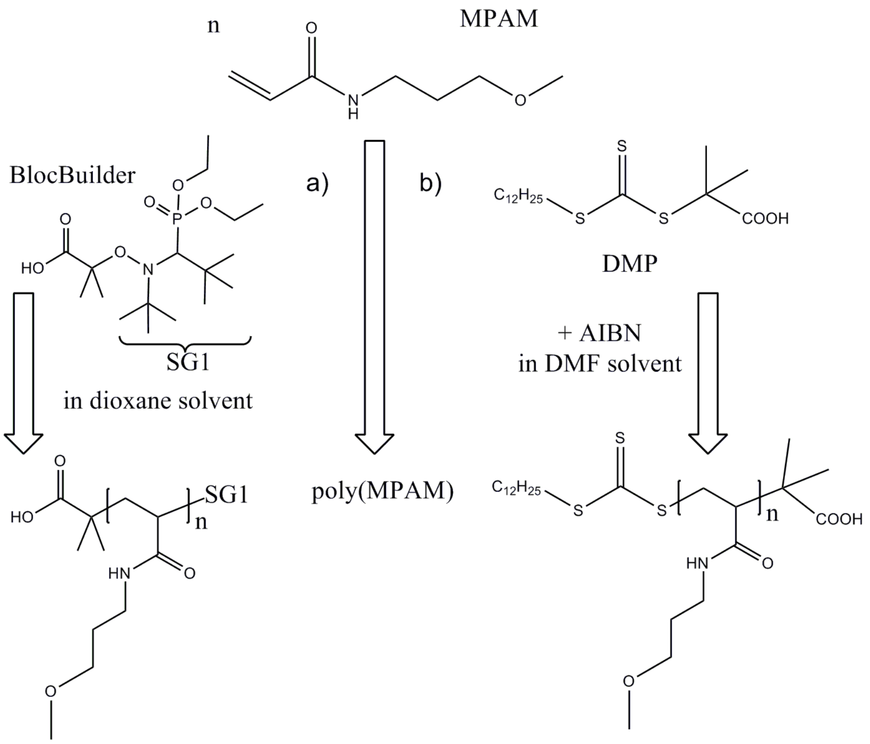

Scheme 3- 1 Reaction pathway for *N*-(3-methoxypropyl) acrylamide (MPAM) homopolymerizations by (a) nitroxide mediated radical polymerization (NMP) using 2-([*tert*-butyl[1-(diethoxyphosphoryl)-2,2-dimethylpropyl]amino]oxy)-2-methylpropanoic acid (BlocBuilder) alkoxyamine in 50 wt% 1,4-dioxane solvent; (b) reversible addition−fragmentation chain transfer radical polymerization (RAFT) using 2,2'-azobisisobutyronitrile (AIBN) initiator and 2-dodecylsulfanylthiocarconylsulfanyl-2-methylpropionic acid (DMP) chain transfer agent in 50 wt% *N*,*N*-dimethylformamide (DMF) solvent.

3.2 Experimental Section

3.2.1 Materials

The RAFT chain transfer agent (CTA) trithiocarbonate 2-dodecylsulfanylthiocarconylsulfanyl-2-methylpropionic acid (DMP, Sigma Aldrich), lithium bromide (ReagentPlus, ≥ 99%, Sigma Aldrich), *N*-(3-methoxypropyl) acrylamide (MPAM, 95%, contains 100 – 500 ppm monomethyl ether hydroquinone as stabilizer, Sigma Aldrich), *N*,*N*-diethylacrylamide (DEAAM, > 95%, contains 100 ppm monomethyl ether hydroquinone as stabilizer, Polysciences), 2-([*tert*-butyl[1-(diethoxyphosphoryl)-2,2-dimethylpropyl]amino]oxy)-2-methylpropanoic acid (BlocBuilder, 99%, Arkema), [*tert*-butyl[1-(diethoxyphosphoryl)-2,2-dimethylpropyl]amino]oxidanyl (SG1, > 85%, Arkema) were used as received. The deuterated chloroform ($CDCl_3$, > 99%, Cambridge Isotopes Laboratory), *N*,*N*-dimethylformamide (DMF, > 95% certified ACS, and 99.5% HPLC grade, Acros Organics), 1,4-dioxane (≥ 99%, certified ACS Reagent Grade, Fisher Scientific), ethyl ether anhydrous (> 95%, BHT stabilized/certified ACS, Fisher Scientific) were also used as received. 2,2'-azobisisobutyronitrile (AIBN, Vazo 67 from Du Pont) was recrystallized from methanol. 2-Methyl-2-[*N*-*tert*-butyl-*N*-(1-diethoxyphosphoryl-2,2-dimethylpropyl)aminoxy]-*N*-propionyloxysuccinimide (NHS-BlocBuilder) was synthesized according to literature[110]. *N*-*tert*-Butyl-*N*-(2-methyl-1-phenylpropyl)-*O*-(1-phenylethyl)hydroxylamine NMP initiator (PhEt-TIPNO) was used as received from Aldrich.

3.2.2 Polymer Synthesis

General Procedure

All polymerizations (Scheme 3-1) were performed in a three-neck round bottom flask (10 ml) equipped with a condenser, capped with a rubber septum with needle inserted to relieve the nitrogen purge, temperature well with thermocouple, and a magnetic stir bar. A thermocouple was connected to a temperature controller, which was used to regulate the temperature of the reaction mixture using a heating mantle. The condenser was cooled using an Isotemp 3016D (Fisher Scientific) chiller unit in order to prevent any monomer or solvent evaporation during the reaction. The solution was bubbled with nitrogen for 20 min before the reaction, and the purge was present throughout the entirety of the reaction with reduced flow rate. The time at which the temperature in the reactor reached the set point was taken as t = 0 min. The samples were periodically withdrawn by syringe and precipitated in an excess of cold diethyl ether. The excess of solvent was decanted to recover the crude polymer, which was then dried in a vacuum oven at 40 °C overnight.

General NMP Homopolymerization

All polymerizations were conducted with unimolecular alkoxyamine BlocBuilder in 1,4-dioxane (50 wt%) at 90 or 110 °C. The molar ratio of additional SG1 relative to BlocBuilder (r = $[SG1]_0/[BlocBuilder]_0$) was either 0 or 0.1, and the target DP_n at complete conversion was calculated to be 140, 210 or 349 (corresponding to molecular weights of 20, 30 or 50 kg mol^{-1}, respectively). The formulation of $MPAM_{349}$-0-110 is given as an example (Table 3-1). BlocBuilder (0.030 g, 0.079 mmol), MPAM (4.02 g, 28.11 mmol), 1,4-dioxane (4.00 g, 45.45 mmol) were added to the reactor. The polymerization was performed at 110 °C for 7 h. The final yield was 1.17 g (24% conversion with $\overline{M_n}$ = 14.9 kg mol^{-1} and Đ = 1.48). The molecular weight data was obtained by gel permeation chromatography (GPC) in DMF solvent at 50 °C relative to PMMA standards (see *Characterization* section).

General RAFT Homopolymerization

All polymerizations were conducted with AIBN as the initiator and DMP as the chain transfer reagent in DMF (50 wt% solution) at 60 or 75 °C. The molar ratio of DMP relative to AIBN (R = $[DMP]_o/[AIBN]_o$) ratio was either 5:1 or 10:1, and the target DP_n at complete conversion was calculated to be 105, 175, or 349 (corresponding to molecular weight of 15, 25 or 50 kg mol^{-1}, respectively). A typical procedure for $MPAM_{175}$-10-75 is described below (Table 3-2). AIBN (0.0020 g, 0.0122 mmol), DMP (0.0444 g, 0.1218 mmol), MPAM (3.01 g, 20.99 mmol), DMF (3.00 g, 41.09 mmol) were added to the reactor. The polymerization was performed at 75 °C for 3 h. The final yield was 0.94 g (67% conversion with $\overline{M_n}$ = 15.6 kg mol^{-1} and Đ = 1.31). In general, diethyl ether worked quite well to recover the final polymer; however the yield was lower than expected in this particular example. The molecular weight data was obtained by gel permeation chromatography (GPC) in DMF solvent at 50 °C relative to PMMA standards (see *Characterization* section).

Table 3- 1 Experimental conditions for poly(*N*-(3-methoxypropyl) acrylamide) (poly(MPAM)) homopolymers synthesized by nitroxide mediated radical polymerization.

Experimental ID[a]	[BlocBuilder]$_0$ (mol L^{-1})	[SG1]$_0$ (mol L^{-1})	r[b]	[MPAM]$_0$ (mol L^{-1})	[Dioxane]$_0$[c] (mol L^{-1})	T (°C)	DP$_{n,target}$
MPAM_{140}-0-90	0.0249	0.0000	0.0	3.54	5.91	90	140
MPAM_{140}-0.1-90	0.0260	0.0026	0.1	3.64	5.75	90	140
MPAM_{210}-0-90	0.0174	0.0000	0.0	3.58	5.85	90	210
MPAM_{210}-0-110	0.0171	0.0000	0.0	3.60	5.82	110	210
MPAM_{210}-0.1-110	0.0169	0.0017	0.1	3.62	5.78	110	210
MPAM_{349}-0-110	0.0101	0.0000	0.0	3.60	5.82	110	349
Experimental ID[a]	**[Initiator]$_0$ (mol L^{-1})**	**Initiator[d]**		**[MPAM]$_0$ (mol L^{-1})**	**[DMF]$_0$[c] (mol L^{-1})**	**T (°C)**	**DP$_{n,target}$**
MPAM_{175}-0-110-BB	0.0197	BB		3.44	6.74	110	175
MPAM_{175}-0-110-NHSBB	0.0198	NHS-BB		3.44	6.73	110	174
MPAM_{175}-0-110-PhEtTIPNO	0.0197	PhEt-TIPNO		3.46	6.70	110	176

[a] Experimental identification (ID) for MPAM homopolymerizations are given by MPAM_X-Y-Z, with MPAM representing *N*-(3-methoxypropyl) acrylamide, X representing the DP$_{n,target}$ used, Y representing the ratio *r*, and Z representing the set point temperature. [b] Initial molar ratio of SG1 free nitroxide to BlocBuilder alkoxyamine used in NMP homopolymerization (*r* = [SG1]$_o$/[BlocBuilder]$_o$). [c] All homopolymerizations were done in 50 wt% solvent solution. [d] Different initiators were used, where BB is BlocBuilder, NHS-BB is NHS-BlocBuilder, and PhEt-TIPNO is styryl-TIPNO alkoxyamines.

Chain Extension Experiment

Chain extension using MPAM_{105}-5-75 as a macroinitiator and a fresh batch of *N*,*N*-diethylacrylamide (DEAAM) is used as an example (Table 3-2). The chain extension experiments were performed by addition of a fresh monomer batch to maintain the total concentration of monomers plus macroinitiator at 50 wt% in the solution. In the reactor, MPAM_{105}-5-75 homopolymer (0.58 g, 0.04 mmol, $\overline{M_n}$ = 14.4 kg mol^{-1}, Đ = 1.23), DEAAM (0.79 g, 6.22 mmol), AIBN (0.005 g, 0.03 mmol) and DMF (1.3 g, 18.06 mmol) were mixed. The chain extension was performed at 75 °C for 12 h, and the target DP$_n$ for the second block at complete conversion was calculated to be 154 (corresponding to 19.5 kg mol^{-1}), however one has to note that the molecular weight of the macroinitiator is relative to PMMA standards (see *Characterization* section). The block copolymer was recovered by precipitation in diethyl ether, and the final yield was 0.84 g ($\overline{M_n}$ = 22.3 kg mol^{-1} and Đ = 1.41). The molecular weight data was obtained by gel permeation chromatography (GPC) in DMF solvent at 50 °C relative to PMMA standards (see *Characterization* section).

Table 3- 2 Experimental conditions for poly(*N*-(3-methoxypropyl) acrylamide) (poly(MPAM)) homopolymers and poly(MPAM)-*b*-poly(*N,N*-diethylacrylamide) block copolymer synthesized by reversible addition−fragmentation chain transfer radical polymerization.

Experimental ID[a]	**$[AIBN]_0$ (mol L^{-1})**	**$[DMP]_0$ (mol L^{-1})**	**R**[b]	**$[MPAM]_0$ (mol L^{-1})**	**$[DMF]_0$**[c] **(mol L^{-1})**	**T (°C)**	**$DP_{n,target}$**
$MPAM_{349}$-5-60	0.0020	0.0099	5.0	3.44	6.74	60	349
$MPAM_{175}$-5-60	0.0045	0.0193	4.3	3.44	6.73	60	175
$MPAM_{175}$-10-75	0.0020	0.0200	10.0	3.44	6.74	75	175
$MPAM_{175}$-5-75	0.0040	0.0201	5.1	3.46	6.71	75	175
$MPAM_{105}$-5-75	0.0067	0.0336	5.05	3.44	6.74	75	105
Experimental ID[a]	**$[Macroinitiator]_0$ (mol L^{-1})**		**$[AIBN]_0$ (mol L^{-1})**	**$[DEAAM]_0$ (mol L^{-1})**	**$[DMF]_0$**[c] **(mol L^{-1})**	**T (°C)**	**$DP_{n,target}$**[d]
$MPAM_{105}$-5-75/DEAAM	0.018		0.0134	2.74	7.96	75	154

[a] Experimental identification (ID) for MPAM homopolymerizations are given by $MPAM_X$-Y-Z, with MPAM representing *N*-(3-methoxypropyl) acrylamide, X representing the $DP_{n,target}$ used, Y representing the ratio *R*, and Z representing the set point temperature. Experimental identification (ID) for chain extensions is given by $MPAM_X$-Y-Z/DEAAM with $MPAM_X$-Y-Z representing the experimental identification for the macroinitiator used in the synthesis and DEAAM representing *N,N*-diethylacrylamide, the monomer which was polymerized. [b] Initial molar ratio of DMP chain transfer agent to AIBN initiator used in RAFT homopolymerization ($R = [DMP]_o/[AIBN]_o$). [c] All polymerizations were done in 50 wt% DMF solution. [d] The target DP_n of the second block.

3.2.3 Polymer characterization

Nuclear Magnetic Resonance Spectroscopy (NMR)

The samples taken during polymerization were analysed with ^1H NMR spectroscopy (300MHz Varian Gemini) in $CDCl_3$ in order to track the progression of the polymerization. Monomer conversion *(X)* was determined by comparing the area associated to the vinylic protons of the monomer (δ = 6.1 and 5.6 ppm, $C\mathbf{H_2}CHNH$, each peak corresponding to 1H) to the area associated to the protons in the amide tail (δ = 3.29 - 3.46 ppm, $HNC\mathbf{H_2}CH_2C\mathbf{H_2}OC\mathbf{H_3}$, corresponding to 7H in total).

Gel Permeation Chromatography (GPC)

The number average molecular weight, $\overline{M_n}$, and the dispersity, Đ, were determined by gel permeation chromatography (GPC, Water Breeze). The GPC was equipped with 2 ResiPore (3 μm, MULTI pore type, 250 mm x 4.6 mm) columns with a ResiPore guard column (3 μm, 50 mm x 4.6 mm) from Polymer Laboratories. HPLC grade DMF with 1 g l^{-1} of lithium bromide was used as a mobile phase with a flow rate of 0.3 ml min^{-1}. The columns were heated to 50 °C during the analysis and the molecular weights were determined by calibration of GPC relative to poly(methyl methacrylate) (PMMA) standards. GPC was equipped with ultra-violet (UV 2487) and differential refractive index (RI 2414) detectors.

UV-Vis Spectroscopy

The cloud point temperatures (CPTs) of poly(MPAM) homopolymers were measured by UV-Vis spectroscopy using a Cary 5000 UV−Vis−NIR spectrometer (Agilent Technologies) equipped with a temperature controlled Peltier thermostatted (6 × 6) multicell holder. The light absorbance was measured at a wavelength of 500 nm and a heating rate of 1 °C min^{-1} from 60 to 99 °C. The CPT was determined as the temperature at which the normalized transmittance reached 50% on a heating cycle.

Dynamic Light Scattering (DLS)

The CPTs of poly($MPAM_{105}$-5-75)-*b*-poly(DEAAM) block copolymer were estimated using the Malvern Zetasizer Nano ZS equipped with a 633 nm red laser. All DLS measurements were performed at a scattering angle (θ) of 173°. The samples were filtered using a 0.2 micron filter and then heated in increments of 1 °C, followed by 18 measurements, which were averaged together to give one value at the corresponding temperature. For more reliable measurement of the hydrodynamic radius, the refractive index (RI) of a sample has to be estimated. The RI of 1.4923 was used, which corresponds to PMMA at 20 °C for $\lambda = 578$ nm.[111]

For the stability analysis, a sample was held at a temperature above its CPT (80 °C for poly($MPAM_{105}$-5-75)-*b*-poly(DEAAM) block copolymer at 2 wt% solution concentration) for 15 hours. The interval between the measurements was set to be 30 minutes, and there were a total of 30 measurements.

3.3 RESULTS AND DISCUSSIONS

3.3.1 Homopolymerization by NMP

A series of MPAM homopolymerizations by NMP using BlocBuilder as the unimolecular initiator and additional SG1 free nitroxide were performed as a function of temperature, various target DP_n and the initial ratio of SG1 to BlocBuilder (see all the formulations listed in Table 3-1). The characteristic kinetic plots of log $((1-X)^{-1})$ (X = conversion) versus time are shown in Figure 3-1a. For all cases studied, there are conversions of about 10 – 20 % at t = 0, indicating the presence of fast polymerization before the set temperature was reached. The conversion stayed relatively constant throughout the polymerization, and the plateau indicates the presence of termination reactions. For some of the formulations there was almost no polymer obtained. For the experiments shown in Figure 3-1c, the $\overline{M_n}$ stays constant for reactions involving additional SG1 and low target DP_n. For the formulations with no additional SG1 and with higher target molecular weight ($MPAM_{349}$-0-110), the experimental $\overline{M_n}$ increases with conversion, but it is just slightly higher than the theoretical prediction. This may be due to measuring $\overline{M_n}$ relative to PMMA standards (see *Characterization* section) or irreversible termination. In literature there are cases of chain transfer to monomer[105, 112] and solvent[105, 113] reactions, resulting in downward deviation of the linearity for the molecular weight plots versus conversion. Here, the dispersities for all of the experiments were somewhat high (Figure 3-1b, Đ ~ 1.5 - 1.6), and the GPC chromatograms in Figure 3-1d indicate that there was little chain growth beyond very early times, suggesting that the chains were de-activated and not polymerizing in a controlled manner almost from the onset of each polymerization.

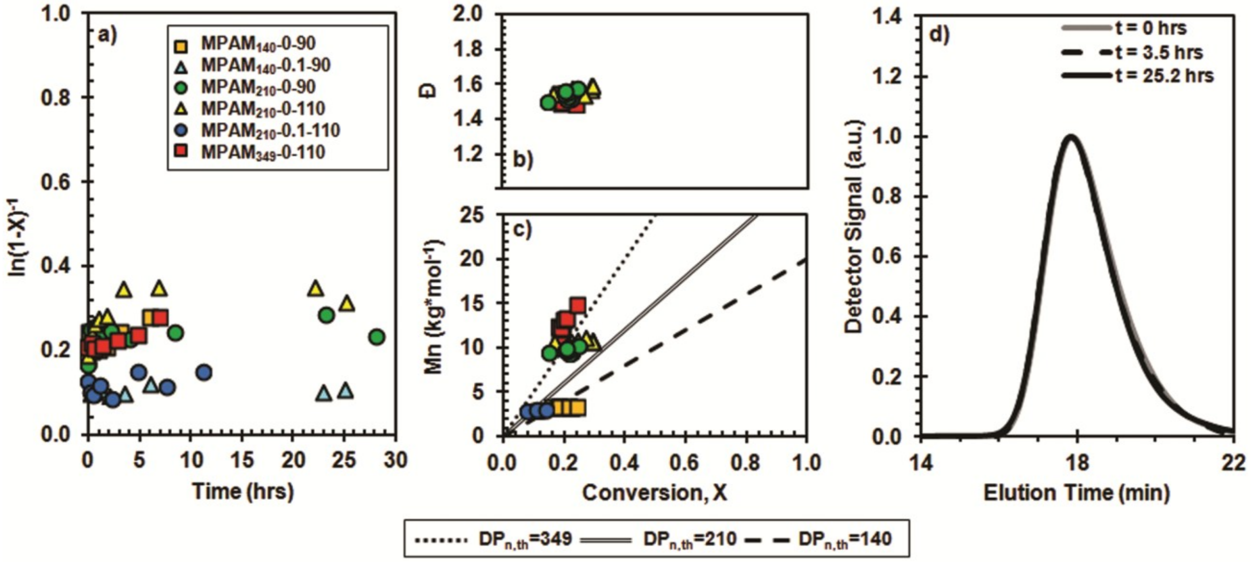

Figure 3- 1 Poly(*N*-(3-methoxypropyl) acrylamide) (poly(MPAM)) characterizations by nitroxide-mediated controlled radical polymerization (NMP): (a) semi-logarithmic plot of conversion ($\ln((1-X)^{-1}$) versus time; (b) Đ versus *X*; (c) $\overline{\boldsymbol{M_n}}$ versus *X;* (d) gel permeation chromatograms of MPAM$_{210}$-0-110 at various times.

Based on the results presented in Figure 3-1, NMP of MPAM using BlocBuilder and SG1 initiators in 1,4-dioxane failed at an early stage of the polymerization, probably due to early termination or chain transfer reactions, as seen from the downwards deviation of the linearity for the molecular weight plots versus conversion. Solvent[114, 115] and initiator[70, 71, 110] selection might play a big role on the polymerization. For instance, Guillaneuf and co-workers used 2,2-diphenyl-3-phenylimino-2,3-dihydroindol-1-yloxyl (DPAIO) - based alkoxyamines for controlled polymerization of methyl methacrylate (MMA) in bulk (Đ = 1.3 - 1.4 at conversions less than 60%), where homopolymerization of methacrylates by NMP traditionally has been hard to control.[70] Similarly, other initiators were synthesized and proved to be more effective than the traditional NMP alkoxyamines.[116] Zetterlund and Aldabbagh groups[115] studied the effect of straight-chain and branched alcohols as solvents on chain transfer to solvent of acrylamide monomers, such as *N*-tert-butylacrylamide (TBAM) and *N*-(2-morpholin-4-ylethyl)acrylamide (MEA). They found that the extent of chain transfer to solvent depended on the length of the carbon-carbon chain in the case of linear alcohol solvents, and it was the smallest for a highly branched alcohol.[115] On the contrary, Dire et al.[114] studied the solvent effect on copolymerization of methacrylic acid with a small amount of styrene, and they found that the polymerization rates in both ethanol and 1,4-dioxane were not very different. In this work an effect of different solvent (more polar) and different initiators (Figure 3-2) was investigated.

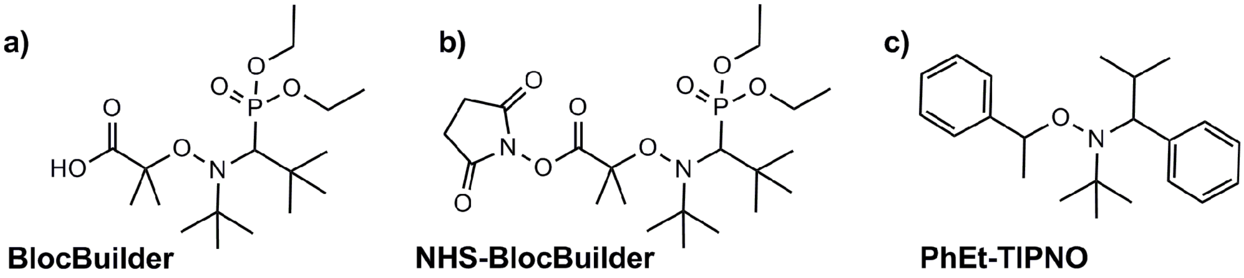

Figure 3- 2 Structures of different alkoxyamines used for nitroxide-mediated controlled radical polymerization: (a) 2-([*tert*-butyl[1-(diethoxyphosphoryl)-2,2-dimethylpropyl]amino]oxy)-2-methylpropanoic acid (BlocBuilder); (b) 2-Methyl-2-[*N*-*tert*-butyl-*N*-(1-diethoxyphosphoryl-2,2-dimethylpropyl)aminoxy]-*N*-propionyloxysuccinimide (NHS-BlocBuilder); (c) *N*-*tert*-Butyl-*N*-(2-methyl-1-phenylpropyl)-*O*-(1-phenylethyl) (PhEt-TIPNO).

Figure 3-3 shows the results for MPAM polymerizations initiated either by BlocBuilder, NHS-BlocBuilder or styryl-TIPNO initiators, in DMF solvent. Substituting 1,4-dioxane solvent with DMF did not show any effect on polymerization as $MPAM_{175}$-0-110-BB had ~ 20 % conversion during the initial stage with no significant chain growth at later times. There was no increase in conversion when styryl-TIPNO was used as an initiator ($MPAM_{175}$-0-110-PhEtTIPNO). Molecular weight data revealed that there was low initiator efficiency since high molecular weight chains were present at an early stage of the polymerization, and $\overline{M_n}$ decreased with conversion. Lastly, $MPAM_{175}$-0-110-NHSBB had a linear increase of conversion with time at low conversions, with $\overline{M_n}$ following the theoretical line until about 40% conversion. NHS-BlocBuilder has a very high dissociation constant (k_d) (5 s^{-1} for NHS-BlocBuilder[110] compared to 0.32 s^{-1} for BlocBuilder[110] and 3.3×10^{-3} s^{-1} for PhEt-TIPNO[117] at 120 °C), and relatively lower activation energy (105 kJ mol^{-1} for NHS-BlocBuilder[110] compared to 112 kJ mol^{-1} for BlocBuilder[110] and 129.6 kJ mol^{-1} for PhEt-TIPNO[117] at 120 °C). It has been shown that the value of the initiating dissociation rate constant plays a prominent role in the success of NMP polymerization.[70, 118] Having a much higher dissociation constant, NHS-BlocBuilder provides excess SG1 nitroxide from the onset of polymerization that could help to control MPAM homopolymerization.

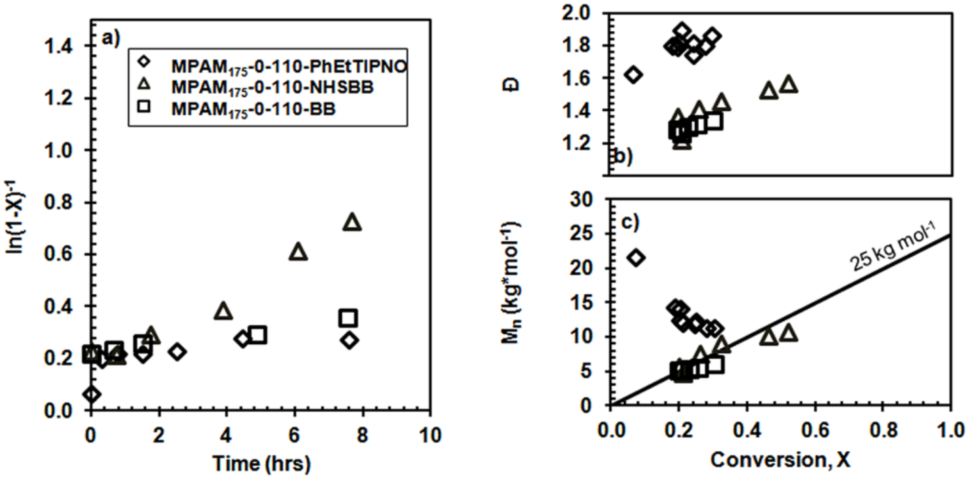

Figure 3- 3 Poly(*N*-(3-methoxypropyl) acrylamide) (poly(MPAM)) characterizations by nitroxide-mediated controlled radical polymerization using different initiators: (a) semi-logarithmic plot of conversion ($\ln((1-X)^{-1})$) versus time; (b) Đ versus X; (c) $\overline{\boldsymbol{M_n}}$ versus X, where 2-([*tert*-butyl[1-(diethoxyphosphoryl)-2,2-dimethylpropyl]amino]oxy)-2-methylpropanoic acid (BlocBuilder), 2-Methyl-2-[*N*-*tert*-butyl-*N*-(1-diethoxyphosphoryl-2,2-dimethylpropyl)aminoxy]-*N*-propionyloxysuccinimide (NHS-BlocBuilder), *N*-*tert*-Butyl-*N*-(2-methyl-1-phenylpropyl)-*O*-(1-phenylethyl) (PhEt-TIPNO).

MPAM monomer structure has a secondary amine functionality, and monomers with similar functionality were shown to be less stable and less reactive than the monomers with tertiary amine functionality, probably due to stronger electron-donating conjugative effect of the latter.[87] The increased steric hindrance of NHS-BlocBuilder, if compared to BlocBuilder where the carboxylic acid group is not protected, might help to stabilize the radical more and to increase the polymerization rate. For instance, Studer et al. was able to polymerize NIPAM, which has a similar structure to MPAM, in benzene using sterically hindered 2,2,6,6-tetraethylpiperidin-4-on-*N*-oxyl nitroxide and its corresponding alkoxyamine (Đ ~ 1.16 – 1.26).[119] At higher conversions in Figure 3-3, there are mostly termination reactions, as seen from deviation of molecular weight versus conversion from linearity, from the increase of dispersity, and from the sudden increase of conversion. Therefore, NMP of MPAM with NHS-BlocBuilder is possible, however the system lacks control over the molecular weight at higher conversions and more troubleshooting has to be done in order to determine the optimal conditions with such an initiator.

3.3.2 Homopolymerization By RAFT

Table 3-2 lists the experimental conditions for RAFT polymerizations of MPAM, where the effect of temperature, various target DP_n and the initial ratio of DMP to AIBN were examined. The theoretical molecular weight at complete conversion can be calculated from Equation 1.

$$\overline{M_{n,th}} = M_{CTA} + \frac{[monomer]}{[CTA]} * M_{monomer} \qquad \text{(Equation 1)}$$

where M_{CTA} and $M_{monomer}$ are the molecular weight of RAFT agent and monomer, respectively, and [CTA] and [monomer] are initial concentrations of RAFT agent and monomer, respectively. The Equation 1 does not consider the number of radicals derived from other sources than the CTA-derived ones, such as initiator-derived chains.[87, 120]

Unlike NMP, RAFT-synthesized MPAM homopolymers exhibited first order kinetic behavior (Figure 3-4a). At time zero, which was taken when the set temperature was reached, the conversion is only 4 - 7 %, indicating a presence of a controlled system. The conversion increased linearly with time with no signs of termination reactions. The effect of temperature on the reaction rate and control was studied, while keeping the target molecular weight and CTA to initiator ratio constant. It was found that at 60 °C the reaction propagated very slowly with no apparent sign of progression ($MPAM_{175}$-5-60); however, at 75 °C, a much higher conversion of 50% was reached after 45 minutes ($MPAM_{175}$-5-75) (see Figure 3-4a). The $\overline{M_n}$ follows the theoretical line (Figure 3-4b) for all reactions, and the dispersity throughout the synthesis remained within 1.17 - 1.47 (Figure 3-4c). The experimental $\overline{M_n}$ is lower than the theoretical one likely due to the differences in the hydrodynamic volume of PMMA standards used for GPC analysis (see the *Characterization* section). However, a similar behavior was observed for other mono-*N*-substituted acrylamides, where negative deviation of the molecular weight from linearity was likely due to chain transfer to monomer.[87] The GPC traces in Figure 3-4d show clear shifts to lower elution volume (higher molecular weight). The traces at higher conversion have some tailing at higher elution volumes (lower molecular weight), which is likely due to termination reactions present during the initiation and/or propagation steps of the polymerization. All the molecular weight properties of the final homopolymers are summarized in Table 3-3.

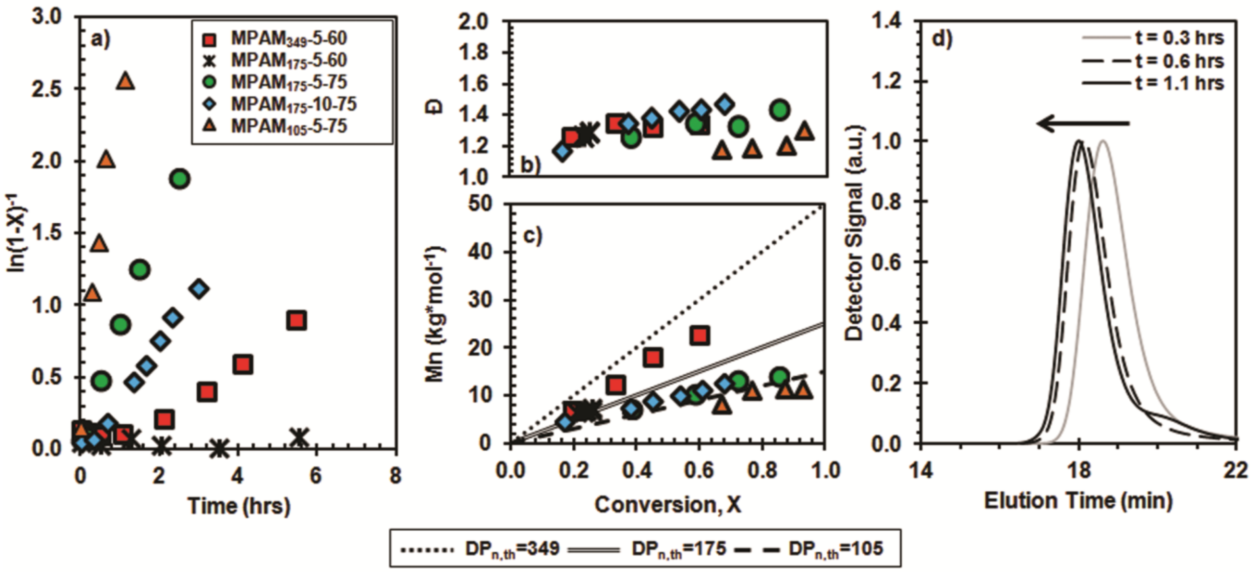

Figure 3- 4 Poly(*N*-(3-methoxypropyl) acrylamide) (poly(MPAM)) characterizations by reversible addition chain-transfer radical polymerization (RAFT): (a) semi-logarithmic plot of conversion ($\ln((1-X)^{-1}$) versus time; (b) Đ versus X; (c) $\overline{M_n}$ versus X; (d) gel permeation chromatograms of MPAM$_{105}$-5-75 at various times.

Table 3- 3 Molecular weight characterization for poly(*N*-(3-methoxypropyl) acrylamide) (poly(MPAM)) homopolymers and block copolymer with *N*,*N*-diethylacrylamide (DEAAM) synthesized by reversible addition chain-transfer radical polymerization in 50 wt% DMF solution.

Experimental ID[a]	X[b]	$\overline{M_n}$[c] (kg mol^{-1})	$\overline{M_w}/\overline{M_n}$[c]	F_{DEAAM}[d]	CPT $_{2\ wt\%}$ (°C)
MPAM$_{349}$-5-60	0.59	25.2	1.27	n/a	75.9
MPAM$_{175}$-5-60	0.25	7.0	1.28	n/a	soluble
MPAM$_{175}$-5-75	0.85	14.3	1.49	n/a	86.6
MPAM$_{175}$-10-75	0.67	15.6	1.32	n/a	81.5
MPAM$_{105}$-5-75	0.92	14.4	1.23	n/a	80.2
MPAM$_{105}$-5-75/DEAAM	n/a[e]	22.3	1.41	0.38	37& 75[f]

[a] Experimental identification for MPAM homopolymerizations are given by MPAM$_X$-Y-Z, with MPAM representing *N*-(3-methoxypropyl) acrylamide , X representing the DP$_{n,targ}$ used, Y representing the ratio *R* (*R* = [DMP]$_o$/[AIBN]$_o$), and Z representing the set point temperature. Experimental identification (ID) for chain extensions is given by MPAM$_X$-Y-Z/DEAAM with MPAM$_X$-Y-Z representing the experimental identification for the macroinitiator used in the synthesis and DEAAM representing *N*,*N*-diethylacrylamide, the monomer which was polymerized. [b] Monomer conversion determined by ^{1}H NMR spectroscopy. [c] Number-average molecular weight ($\overline{M_n}$) and molecular weight distribution ($\overline{M_w}/\overline{M_n}$) were determined by gel permeation chromatography (GPC). [d] F_{DEAAM} is the molar fraction of DEAAM in the final block copolymer as determined by ^{1}H NMR spectroscopy. [e] The chain extension was not monitored for conversion. [f] As determined by dynamic light scattering (DLS)

3.3.3 Block Copolymer Synthesis via RAFT.

The ability of the resulting poly(MPAM) homopolymer to re-initiate a fresh batch of monomer was investigated. The formulation for chain-extension of MPAM_{105}-5-75 homopolymer with *N*,*N*-diethylacrylamide (DEAAM) is listed in Table 3-2. The shift of the GPC traces to a lower elution volume indicates growth from the macroinitiator towards a higher molecular weight polymer (Figure 3-5). The Đ of the final block was 1.41, which is broader than that of the macroinitiator (Đ = 1.23) although the peak of the chain-extended species was monomodal with some tailing indicating a very low fraction of unreacted macroinitiator remained. The final molecular weight data (relative to PMMA standards in DMF at 50 $^{\circ}$C, see *Characterization* section) can be found in Table 3-3.

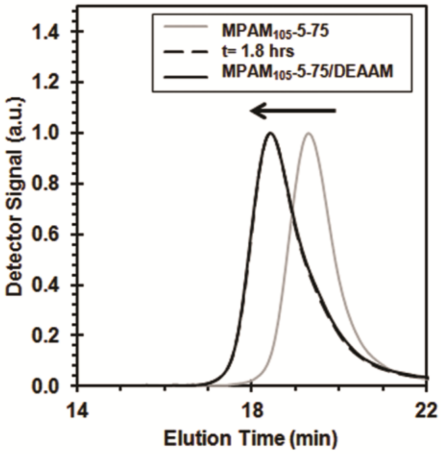

Figure 3- 5 Gel permeation chromatograms (GPC) of *N*,*N*-diethylacrylamide (DEAAM) chain extension done in 50 wt% solution in DMF at 75 °C from MPAM_{105}-5-75 macroinitiator.

3.3.4 Thermo-Responsive Behavior of Homopolymers in Water.

The MPAM homopolymers were tested for thermo-responsive behaviour in aqueous media. Ito[109] reported a cloud point of 44.5 °C for poly(MPAM) in 1 % solution, but no molecular weight data was shown. Yamazaki et al. also studied the thermo-responsive behavior of poly(MPAM) homopolymers, and they did not observe any phase transition up to 0.1 wt% when the solution was heated up to 60 °C (M_n ~ 2 kg mol^{-1} as determined by an acid-base titration of the terminal carboxyl groups).[108] Both groups used conventional radical polymerization in order to get the desired homopolymers, and it is possible to speculate that the discrepancy is due to lack of control over the microstructure of the final polymer or, in the latter case, the polymers are water-soluble due to low molecular weight. The LCST and phase transition highly depend on molecular weight distribution.[39, 47-49] Monomodal and narrow molecular weight distribution are essential in order to obtain sharp response during phase transition; therefore, only polymer samples obtained by RAFT polymerization were considered for the subsequent analysis.

In our study, the range of the molecular weights observed was relatively narrow (14.3 - 25.2 kg mol^{-1}) and the CPT was found to be a weak function of molecular weight with no particular trend in the CPT values with the increase of $\overline{M_n}$. Weak molecular weight dependence for the similar range of molecular weights was also observed in the case of homopolymers of 2-(dimethylamino)ethyl methacrylate (DMA) and 2-(*N*-morpholino)ethyl methacrylate (MEMA) homopolymers, where there was only 4 – 5 °C difference in CPTs.[121] The same study also looked at a wider range of $\overline{M_n}$'s (from 1×10^3 to 5×10^4 g mol^{-1} and from 1×10^3 to 3×10^4 g mol^{-1} for DMA and MEMA homopolymers, respectively), and the CPT was found to be also sensitive of molecular weight (the difference in CPTs was 14 - 19 °C over the ranges provided above, which corresponds to about 0.3 - 0.7 °C change in CPT values per 1 kg mol^{-1}).[121] Hence, a similar behavior might be observed in our study if a wider range of $\overline{M_n}$ was regarded. For instance, the CPTs were in the range of 77.8 to 90.9 ^{o}C for 1 wt%, and 75.9 to 86.6 ^{o}C for 2 wt% solution concentration (13 and 11 °C difference, respectively, which corresponds to 1 - 1.2 °C change in CPT values per 1 kg mol^{-1}).

The dependence of CPT on the heating rate is well studied in literature[76, 78, 86, 97, 122] For instance, our group studied the effect of heating rate on transition of poly(2-*N*-morpholinoethyl methacrylate-*ran*-9-(4-vinylbenzyl)-9H-carbazole (poly(MEMA-*ran*-VBK))[122] and poly (*N*-(2-methacryloyloxyethyl) pyrrolidone-*stat*-9-(4-vinylbenzyl)-9H-carbazole) **(**poly(MAEPYR-*stat*-VBK))[97] copolymers. As the heating rate was increased from 0.2 to 4 °C min^{-1}, the CPT for poly(MAEPYR-*stat*-VBK) samples (1 wt% concentration) increased from 39.8 °C to 45.2 °C.[97] Similarly, CPT increased by 11 °C for PNIPAM[78] (with the heating rate increase from 0.02 to 5 °C min^{-1}) and by 6 °C for poly(*N*,*N*-diethylacrylamide) (DEAAM)[86] (with the heating rate ranging from 0.06 to 5°C min^{-1}). Here, a heating rate of 1 °C min^{-1} was applied.

The CPT was found to be a weak function of solution concentration. At higher solution concentration (> 3 wt%) the phase separation was not reversible due to sedimentation of the polymer sample (observed for $MPAM_{175}$-5-75 and $MPAM_{349}$-5-60 at 5 wt% solution concentration). The $MPAM_{349}$-5-60 at 0.5 wt% was completely soluble for the range of temperatures studied (25 - 95 °C); therefore, concentrations of less than 1 wt% were not examined. Depending on the polymer sample used, poly(MPAM) exhibited a difference of as much as 9.3 °C in CPTs with the change in solution concentration (from 90.9 °C at 1 wt% solution concentration to 89.7 °C at 3 wt% solution concentration for $MPAM_{175}$-10-75 ($\overline{M_n}$ = 15.6 kg mol^{-1} and Đ = 1.31)). Weak solution concentration dependence was also observed in the case of copolymers of 2-(2-methoxyethoxy)ethyl methacrylate and oligo(ethylene glycol) methacrylate, where the CPT was found to only increase by a few degrees with high dilution.[123]

The solution properties of the resulting MPAM homopolymers were studied in order to confirm the LCST properties of the polymer. The CPT was found to be dependent on the nature of the polymer (eg. there is weak dependence on molecular weight of about 1-1.2 °C change per 1 kg mol^{-1}), the heating rate and the solution concentration (on average, ~ 1-5 °C change in CPT values per 1 wt% change in solution concentration).

3.3.5 Thermal Transition of the Block Copolymer

Two techniques were used to report cloud point temperature (CPT) of a block copolymer: UV-Vis spectroscopy and dynamic light scattering (DLS). UV-Vis measures light transmittance, and it is indicative of the phase transition when the solution turns cloudy, which is mostly due to macroscopic phase separation.[78] DLS, on the other hand, can detect a collapse of a single polymer chain, which is an indicator for the onset of macroscopic phase separation.[78] Figure 3-6 shows the results of the turbidity and light scattering measurements.

More than one transition can be obtained by controlling the architecture of the polymer (eg. by using a block copolymer with distinctive phase transitions corresponding to each block). In this study, the poly(MPAM) homopolymer was chain-extended with DEAAM, which was shown to be easily controlled by NMP.[124] Charleux et al.[124] used BlocBuilder/SG1 initiators for DEAAM synthesis in toluene (Đ < 1.4). Poly(DEAAM) is a temperature responsive acrylamide polymer with LCST around 32-33 °C, similar to that of poly(NIPAM).[87] Since poly(MPAM) was shown to have a rather high LCST, a DEAAM monomer was chosen for chain extension experiment in order to yield a block copolymer with two distinct and easily detectable temperature-responsive blocks. Figure 3-6 shows the results obtained by both UV-Vis (Figure 3-6a) and DLS (Figure 3-6b) as the 2 wt% polymer solution was heated (at 1 °C min^{-1}) from 25 to 95 °C. The macroinitiator (MPAM_{105}-5-75) for the block copolymer was used as a control in both cases. For the block copolymer, UV-Vis was able to detect a small change in transmittance around 40 °C as the solution turned bluish (indicating micellization), and during heating to 95 °C the transmittance dropped to 40 % around 80 °C, the point where the macroinitiator had a phase transition. At this point, the solution became white and more opaque, probably as a result of gross micelle aggregation. DLS was able to detect the first transition around 37 °C as well (increase of R_h from ~ 10 to 20 nm), a point where micelles started to form from hydrated chains. The micelles' R_h is fairly small, which is reasonable considering the $\overline{M_n}$ of the copolymer. The second transition occurred at a lower temperature as expected if compared to UV-Vis results. Macroscopic phase-separation is a slower process, and it requires more time (hence the temperatures are higher for UV-Vis measurements).[78] The second transition, as observed by DLS, occurred around 84 °C, the point where the macroinitiator had a similar phase transition (R_h ~ 100 - 150 nm for the block copolymer and ~ 4200 - 4300 nm for the macroinitiator). The second transition is more diffusive if compared to the macroinitiator, which is probably due to changes in the overall block copolymer solubility[79] and/or dispersity (Đ = 1.23 for MPAM_{105}-5-75 macroinitiator vs Đ = 1.41 or for MPAM_{105}-5-75/DEAAM block copolymer). When the temperature was above the CPT of the macroinitiator, the block copolymer formed stable micelles, since the hydrodynamic radius (R_h) remained quite constant, as opposed to the macroinitiator itself, where particle aggregation and sedimentation were observed.

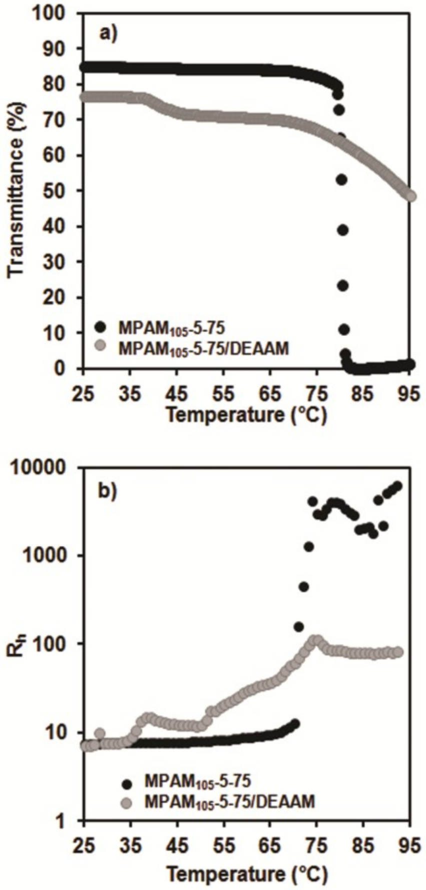

Figure 3- 6 Temperature dependence of (a) the transmittance as measured by UV-Vis during the heat cycle and (b) average hydrodynamic radius (R_h) as measured by DLS during the heat cycle of $MPAM_{105}$-5-75 macroinitiator (black circles, $\overline{\boldsymbol{M_n}}$= 14.4 kg mol^{-1}, Đ = 1.23) and $MPAM_{105}$-5-75/DEAAM block copolymer (grey circles, $\overline{\boldsymbol{M_n}}$= 22.3 kg mol^{-1}, Đ = 1.41, F_{DEAAM} = 0.38) both in 2 wt% solution.

3.3.6 Stability Analysis

The changes in R_h over a 15 hour period at 80 °C for poly(MPAM) homopolymer (empty triangles in Figure 3-7) indicated that the system was not stable. The particle aggregation occurred rapidly since the R_h is very high at early times of the stability experiment. During the experiment the remaining chains were slowly settling as well since there is scatter in the data, and at the end of the experiment the polymer settled at the bottom of the vial, which suggested that macrophase separation had occurred[39]. On the other hand, the changes in R_h are less profound for poly(MPAM)-*b*-DEAAM block copolymer (shown as grey triangles in Figure 3-7) indicating that the micelles formed were relatively stable.

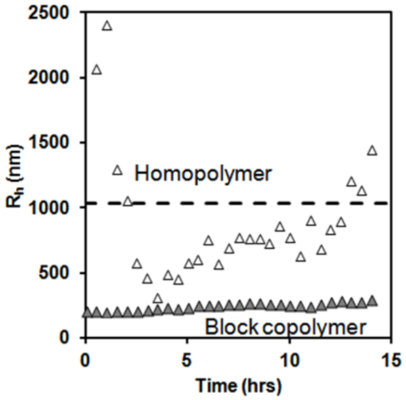

Figure 3- 7 Time dependence of the hydrodynamic radius (R_h) of 2 wt% homopolymer (poly(MPAM), empty triangles, $\overline{M_n}$ = 14.4 kg mol^{-1}, Đ = 1.23) and block copolymer (poly(MPAM)-*b*-DEAAM, grey triangles, $\overline{M_n}$ = 22.3 kg mol^{-1}, Đ = 1.41, F_{DEAAM} = 0.38) solutions at a constant temperature of 80 °C.

3.4 Conclusion

Controlled radical polymerizations were used to study the effect of molecular weight distribution on the LCST behavior of poly(MPAM) in aqueous solution. The nitroxide mediated polymerization with the BlocBuilder/SG1 initiating system was first applied to synthesis of MPAM homopolymers. Under the conditions studied, the polymerizations were limited in conversion with a significant indication of termination reactions (high Đ ~ 1.5 - 1.6 and no growth in chains beyond a conversion of 25 – 30 %). The effect of initiator was studied on MPAM homopolymerizations, and it was found that the succinimidyl ester functionalized BlocBuilder initiator (NHS-BlocBuilder) was able to successfully polymerize MPAM up to about 30 % - 40 % conversion (Đ ~ 1.2 - 1.4); however, at higher conversion, molecular weight deviated from linearity and the final polymer had high Đ. In contrast to NMP, RAFT was far more effective, with linear $\overline{M_n}$ versus X plots (up to 60 - 90 % conversion), low Đ ~ 1.2 - 1.4 and the ability to re-initiate a fresh batch of monomer. Thermoresponsive behavior of poly(MPAM) homopolymers (with $\overline{M_n}$ = 14.3 - 25.2 kg mol^{-1}) in aqueous media was studied at heating rate of 1 °C min^{-1}, and LCSTs were found between 73 and 92 °C depending on solution concentration (1 - 2 wt%). The block copolymer with *N*,*N*-diethylacrylamide (DEAAM) as the second block (poly(MPAM)-*b*-poly(DEAAM) with $\overline{M_n}$= 22.3 kg mol^{-1}, Đ = 1.41, F_{DEAAM} = 0.38) revealed dual LCSTs, where distinctive CPTs were found at 75 °C and 37 °C, respectively to each block. The poly(MPAM)-*b*-DEAAM block copolymer formed stable micelles (~ 100 – 150 nm) with prolonged heating, if compared to the homopolymer, where macrophase separation and, finally, precipitation had occurred.

4. General Conclusion

4.1. Summary

The following key findings are noted below:

- Synthesized *N*-(2-methacryloyloxyethyl) pyrrolidone (MAEPYR) monomer to produce water-soluble stimuli-responsive polymers with a fluorescent tag via NMP;
- Developed a method for a controlled synthesis of *N*-(3-methoxypropyl) acrylamide (MPAM) homopolymers by CRP (principally RAFT);
- Used different solvents and initiators to minimize side reactions, which inhibited the chain growth from the onset of NMP of poly(MPAM) and lead to lower than desired degrees of polymerization.;
- Performed chain extension experiments, and synthesized block copolymers with hydrophilic and temperature-responsive blocks;
- Designed the UV-Vis and DLS analysis methods to determine the CPTs of aqueous solutions of polymers and the effect of different parameters on the transition temperature.

4.2. Future Work

To further complete this study, the effect of different functional groups, instead of a pyrrolidone functionality in a methacrylate-based monomer, on CPT should be regarded. Slight variations in a monomer structure could lead to a dramatic dependence of the CPT, and combination of different monomers in a copolymerization experiment would help to tune the CPT even further to a desired temperature.

The amino-containing polymers can be easily protonated and deprotonated, hence the solution behavior of the polymers is altered. The pH study, where the effect of changing pH on CPT can be regarded, will fulfill this work and demonstrate a possible behavior of these polymers in a physiological system.

NMP of acrylamides with secondary amine groups has to be further investigated. The choice of solvent and/or initiator might have a significant impact on the control of the polymerization. A simpler acrylamide or alkoxyalkylacrylamide monomer, such as *N*-isopropylacrylamide, *N*-propylacrylamide or *N*-*tert*-butylacrylamide, could be used as a model. Another way to ease the polymerization is to protect the amino group leading to an acrylamide with a tertiary amine functionality, which are polymerizable by NMP in a controlled manner. Aqueous polymerizations of the acrylamides could be attempted as well, where altering the pH and deprotonation of the monomer could help to control the polymerization.

References

1 M. Szwarc, *Nature* **1956**, *178*, 1168-1169.
2 A. H. E. Müller, K. Matyjaszewski, *Controlled and living polymerizations : methods and materials*. Wiley-VCH, Weinheim, **2009**, pp. 612
3 J. M. G. Cowie, V. Arrighi, *Polymers : chemistry and physics of modern materials*. 3rd ed., CRC Press, Boca Raton, **2008**, pp. 499
4 V. Mishra, R. Kumar, *J. Sci. Res.* **2012**, *56*, 141-176.
5 R. J. Young, P. A. Lovell, *Introduction to Polymers*. 3rd ed., CRC Press, Boca Raton, FL, **2011**.
6 A. Debuigne, R. Poli, C. Jerome, R. Jerome, C. Detrembleur, *Prog. Polym. Sci.* **2009**, *34*, 211-239.
7 M. A. Tasdelen, M. U. Kahveci, Y. Yagci, *Prog. Polym. Sci.* **2011**, *36*, 455-567.
8 A. Goto, Y. Kwak, T. Fukuda, S. Yamago, K. Iida, M. Nakajima, J. Yoshida, *J. Am. Chem. Soc.* **2003**, *125*, 8720-8721.
9 S. Yamago, B. Ray, K. Iida, J. Yoshida, T. Tada, K. Yoshizawa, Y. Kwak, A. Goto, T. Fukuda, *J. Am. Chem. Soc.* **2004**, *126*, 13908-13909.
10 S. Yamago, E. Kayahara, M. Kotani, B. Ray, Y. Kwak, A. Goto, T. Fukuda, *Angew. Chem. Int. Ed.* **2007**, *46*, 1304-1306.
11 B. Charleux, J. Nicolas, O. Guerret, *Macromolecules* **2005**, *38*, 5485-5492.
12 B. Keoshkerian, P. J. MacLeod, M. K. Georges, *Macromolecules* **2001**, *34*, 3594-3599.
13 M. F. Cunningham, M. Xie, K. B. McAuley, B. Keoshkerian, M. K. Georges, *Macromolecules* **2002**, *35*, 59-66.
14 K. Matyjaszewski, T. P. Davis, *Handbook of radical polymerization*. Wiley-Interscience, Hoboken, **2002**, pp. 920.
15 J. Chiefari, Y. K. Chong, F. Ercole, J. Krstina, J. Jeffery, T. P. T. Le, R. T. A. Mayadunne, G. F. Meijs, C. L. Moad, G. Moad, E. Rizzardo, S. H. Thang, *Macromolecules* **1998**, *31*, 5559–5562.
16 F. D. Jochum, L. Borg, P. J. Roth, P. Theato, *Macromolecules* **2009**, *42*, 7854–7862.
17 A. Postma, T. P. Davis, R. A. Evans, G. Li, G. Moad, M. S. O'Shea, *Macromolecules* **2006**, *39*, 5293–5306.
18 S. Perrier, P. Takolpuckdee, C. A. Mars, *Macromolecules* **2005**, *38*, 6770–6774.
19 G. Moad, Y. K. Chong, A. Postma, E. Rizzardo, S. H. Thang, *Polymer* **2005**, *46*, 8458–8468.
20 P. J. Roth, D. Kessler, R. Zentel, P. Theato, *J. Polym. Sci. Part A: Polym. Chem.* **2009**, *47*, 3118.
21 C. Barner-Kowollik, S. Perrier, *J. Polym. Sci. Part A: Polym. Chem.* **2008**, *46*, 5715–5723.
22 J. Ran, L. Wu, Z. Zhang, T. Xu, *Prog. Polym. Sci.* **2014**, *39*, 124-144.
23 Y. C. Tang, Y. W. Ding, G. Z. Zhang, *J. Phys. Chem. B* **2008**, *112*, 8447-8451.
24 B. H. Lessard, X. Savelyeva, M. Maric, *Polymer* **2012**, *53*, 5649-5656.
25 B. Jeong, A. Gutowska, *Trends Biotechnol.* **2002**, *20*, 360-360.
26 B. R. Twaites, C. D. Alarcon, D. Cunliffe, M. Lavigne, S. Pennadam, J. R. Smith, D. C. Gorecki, C. Alexander, *J. Controlled Release* **2004**, *97*, 551-566.
27 D. Roy, J. N. Cambre, B. S. Sumerlin, *Prog. Polym. Sci.* **2010**, *35*, 278-301.
28 N. Lomadze, H. M. Schneider, *Tetrahedron Lett.* **2005**, *46*, 751-754.
29 C. D. H. Alarcon, S. Pennadam, C. Alexander, *Chem. Soc. Rev.* **2005**, *34*, 276-285.

30 E. S. Gil, S. M. Hudson, *Prog. Polym. Sci.* **2004**, *29*, 1173-1222.
31 A. Chilkoti, M. R. Dreher, D. E. Meyer, D. Raucher, *Adv. Drug Delivery Rev.* **2002**, *54*, 613-630.
32 J. Weidner, *Drug Discovery Today* **2001**, *6*, 1239–1241.
33 M. Yamato, C. Konno, A. Kushida, M. Hirose, M. Utsumi, A. Kikuchi, T. Okano, *Biomaterials* **2000**, *21*, 981–986.
34 K. Uchida, K. Sakai, E. Ito, O. H. Kwon, A. Kikuchi, M. Yamato, T. Okano, *Biomaterials* **2000**, *21*, 923–929.
35 Y. Maeda, T. Higuchi, I. Ikeda, *Langmuir* **2000**, *16*, 7503-7509.
36 H. Chang, L. Shen, C. Wu, *Macromolecules* **2006**, *39*, 2325-2329.
37 Y. Ding, X. Ye, G. Zhang, *Macromolecules* **2005**, *38*, 904-908.
38 M. Heskins, J. E. Guillet, *J. Macromol. Sci. Part A: Chem.* **1968**, *2*, 1441-1455.
39 J. Sun, Y. Peng, Y. Chen, Y. Liu, J. Deng, L. Lu, Y. Cai, *Macromolecules* **2010**, *43*, 4041-4049.
40 P. Liu, L. Xiang, Q. Tan, H. Tang, H. Zhang, *Polym. Chem.* **2013**, *4*, 1068-1076.
41 X. Liu, Y. Xu, Z. Wu, H. Chen, *Macromol Biosci.* **2012**, *13*, 147-154.
42 J. Nicolas, Y. Guillaneuf, C. Lefay, D. Bertin, D. Gigmes, B. Charleux, *Prog. Polym. Sci.* **2013**, *38*, 63-235.
43 P. Bilalis, M. Pitsikalis, N. Hadjichristidis, *J. Polym. Sci. Part A: Polym. Chem.* **2006**, *44*, 659-665.
44 H. A. Ravin, A. M. Seligman, J. Fine, *N. Engl. J. Med.* **1952**, *247*, 921-929.
45 U. Karaaslan, M. Parlaktuna, *Prepr. Pap. - Am. Chem. Soc., Div. Fuel Chem.* **2002**, *47*, 355-358.
46 N. Daraboina, P. Linga, *Chem. Eng. Sci.* **2013**, *93*, 387-394.
47 S. Aoshima, H. Oda, E. Kobayashi, *J. Polym. Sci. Part A: Polym. Chem.* **1992**, *30*, 2407-2413.
48 H. Mori, H. Iwaya, A. Nagai, E. T., *Chem. Commun.* **2005**, 4872-4874.
49 P. Liu, H. Xie, H. Tang, G. Zhong, H. Zhang, *J. Polym. Sci. Part A: Polym. Chem.* **2012**, *50*, 3664-3673.
50 K. Matyjaszewski, T. P. Davis, (eds.), *Handbook of Radical Polymerization*. Wiley-Interscience, Hoboken, NJ, **2002**, pp. 920.
51 G. Moad, E. Bicciocchi, M. Chen, J. Chiefari, C. Guerrero-Sanchez, M. Haeussler, S. Houshyar, D. Keddie, E. Rizzardo, S. H. Thang, J. Tsanaktsidis, *ACS Symp. Ser.* **2012**, *1100*, 243-258.
52 G. Moad, E. Rizzardo, S. H. Thang, *Acc. Chem. Res.* **2008**, *41*, 1133-1142.
53 G. Moad, J. Chiefari, Y. K. Chong, J. Krstina, R. T. A. Mayadunne, A. Postma, E. Rizzardo, S. H. Thang, *Polym. Int.* **2000**, *49*, 993-1001.
54 G. Moad, R. T. A. Mayadunne, E. Rizzardo, M. Skidmore, S. H. Thang, *ACS Symp. Ser.* **2003**, *854*, 520-535.
55 M. Cunningham, M. Lin, J. A. Smith, J. Ma, K. McAuley, B. Keoshkerian, M. Georges, *Prog. Coll. Pol. Sci. S.* **2004**, *124*, 88-93.
56 R. B. Grubbs, *Polym. Rev.* **2011**, *51*, 104-137.
57 C. J. Hawker, A. W. Bosman, E. Harth, *Chem. Rev.* **2001**, *101*, 3661-3688.
58 K. Matyjaszewski, N. V. Tsarevsky, *Nat. Chem.* **2009**, *1*, 276–288.
59 K. Matyjaszewski, W. A. Braunecker, *Prog. Polym. Sci.* **2007**, *32*, 93-146.
60 J. Deng, Y. Shi, W. Jiang, Y. Peng, L. Lu, Y. Cai, *Macromolecules* **2008**, *41*, 3007-3014.

61 G. M. Iskander, L. E. Baker, D. E. Wiley, T. P. Davis, *Polym. Chem.* **1998**, *39*, 4165-4169.

62 J. Nicolas, S. Brusseau, B. Charleux, *J. Polym. Sci. Part A: Polym. Chem.* **2010**, *48*, 34-47.

63 B. Lessard, E. J. Ling, M. S. T. Morin, M. Maric, *J. Polym. Sci. Part A: Polym. Chem.* **2011**, *49*, 1033-1045.

64 B. Lessard, M. Maric, *J. Polym. Sci. Part A: Polym. Chem.* **2011**, *49*, 5270-5283

65 C. Zhang, M. Maric, *J. Polym. Sci. Part A: Polym. Chem.* **2013**, *51*.

66 B. H. Lessard, E. J. Ling, M. Maric, *Macromolecules* **2012**, *45*, 1879-1891.

67 B. H. Lessard, M. Maric, *Can. J. Chem. Eng.* **2012**, *91*, 618-629.

68 W. Zhang, Y. Yan, N. Zhou, Z. Cheng, J. Zhu, C. Xia, X. Zhu, *Eur. Polym. J.* **2008**, *44*, 3300-3305.

69 C. Dire, J. Belleney, J. Nicolas, D. Bertin, S. Magnet, B. Charleux, *J. Polym. Sci. Part A: Polym. Chem.* **2008**, *46*, 6333-6345.

70 Y. Guillaneuf, D. Gigmes, S. R. A. Marque, P. Astolfi, L. Greci, P. Tordo, D. Bertin, *Macromolecules* **2007**, *40*, 3108-3114.

71 A. C. Greene, R. B. Grubbs, *Macromolecules* **2010**, *43*, 10320-10325.

72 J. Nicolas, C. Dire, L. Mueller, J. Belleney, B. Charleux, S. R. A. Marque, D. Bertin, S. Magnet, L. Couvreur, *Macromolecules* **2006**, *39*, 8274–8282.

73 J. Nicolas, B. Charleux, O. Guerret, S. Magnet, *Macromolecules* **2004**, *37*, 4453-4463.

74 C. Lefay, J. Belleney, B. Charleux, O. Guerret, S. Magnet, *Macromol. Rapid Commun.* **2004**, *25*, 1215-1220.

75 H. M. L. Lambermont Thijs, R. Hoogenboom, C.-A. Fustin, C. Bomal-D'Haese, J.-F. Ghy, U. S. Schubert, *J. Polym. Sci. Part A: Polym. Chem.* **2009**, *47*, 515-522.

76 H. Y. Liu, X. X. Zhu, *Polymer* **1999**, *40*, 6985-6990.

77 R. Xu, *Particle Characterization: Light Scattering Methods*. Editor, Kluwer Academic, New York, NY, **2002**.

78 C. Boutris, E. G. Chatzi, C. Kiparissides, *Polymer* **1997**, *38*, 2567-2570.

79 C. Zhang, M. Maric, *Polymers* **2011**, *3*, 1398-1422.

80 J. Y. Huang, K. Matyjaszewski, *Macromolecules* **2005**, *38*, 3577-3583.

81 F. J. Hua, X. G. Jiang, D. J. Li, B. Zhao, *J. Polym. Sci. Part A: Polym. Chem.* **2006**, *44*, 2454-2467.

82 I. Idziak, D. Avoce, D. Lessard, D. Gravel, X. X. Zhu, *Macromolecules* **1999**, *32*, 1260-1263.

83 D. Li, W. J. Brittain, *Macromolecules* **1998**, *31*, 3852-3855.

84 X. Savelyeva, B. H. Lessard, M. Maric, *Macromol. React. Eng.* **2012**, *6*, 200-212.

85 J. E. Chung, M. Yokoyama, T. Aoyagi, Y. Sakurai, T. Okano, *J. Controlled Release* **1998**, *53*, 119–130.

86 I. Idziak, D. Avoce, D. Lessard, D. Gravel, X. X. Zhu, *Macromolecules* **1999**, *32*, 1260-1263.

87 Y. Cao, X. X. Zhu, J. T. Luo, H. Y. Liu, *Macromolecules* **2007**, *40*, 6481-6488.

88 A. Laschewsky, E. D. Rekai, E. Wischerhoff, *Macromol. Chem. Phys.* **2001**, *202*, 276-286.

89 Y. Maeda, J. Sakamoto, S. Y. Wang, Y. Mizuno, *J. Phys. Chem. B* **2009**, *113*, 12456-12461.

90 S. Ito, Y. Matsumaru, T. Hirano, S. Ohashi (Japan as represented by Director General of Agency of Industrial Science), United States, US5525334 **Jun 11, 1996**.

91 A. Yamazaki, F. M. Winnik, R. M. Cornelius, J. L. Brash, *Biochim. Biophys. Acta, Biomembr.* **1999**, *1421*, 103-115.

92 F. M. Winnik, A. Adronov, H. Kitano, *Can. J. Chem. Eng.* **1995**, *73*, 2030-2040.
93 L. Lingyun, L. Qingsheng, S. Anuradha, *ACS Symp. Ser.* **2012**, *1120*, 661-676.
94 C. Norton, D. Falk, United States US3747676 A, **Jul 24, 1973**.
95 K. S. Colle, C. A. Costello, R. H. Oelfke, L. D. Talley, J. M. Longo, E. Berluche (E. P. R. Company) United States US5600044 A, **Feb 4, 1997**.
96 Q. A. Acton, *Vinyl compounds - Advances in research and application*. ScholarlyBrief ed., Editor, ScholarlyEditions, **2013**.
97 X. Savelyeva, M. Marić, *J. Polym. Sci. Part A: Polym. Chem.* **2014**, *52*, 2011-2024.
98 C. Boyer, V. Bulmus, T. P. Davis, V. Ladmiral, J. Liu, S. Perrier, *ACS Chem. Rev.* **2009**, *109*, 5402-5436.
99 D. J. Siegwart, J. K. Oh, K. Matyjaszewski, *Prog. Polym. Sci.* **2012**, *37*, 18-37.
100 B. Grassl, G. Clisson, A. Khoukh, L. Billon, *Eur. Polym. J.* **2008**, *44*, 50-58.
101 O. Gibbons, W. M. Carroll, F. Aldabbagh, B. Yamada, *J. Polym. Sci. Part A: Polym. Chem.* **2006**, *44*, 6410-6418.
102 O. Gibbons, W. M. Carroll, F. Aldabbagh, P. B. Zetterlund, B. Yamada, *Macromol. Chem. Phys.* **2008**, *209*, 2434-2444.
103 J. Rigolini, B. Grassl, L. Billon, S. Reynaud, O. F. X. Donard, *J. Polym. Sci. Part A: Polym. Chem.* **2009**, *47*, 6919-6931.
104 P. O’Connor, P. Zetterlund, F. Aldabbagh, *J. Polym. Sci. Part A: Polym. Chem.* **2011**, *49*, 1719–1723.
105 Y. S. Y. Sugihara, P. O’Connor, P. B. Zetterlund, F. Aldabbagh, *J. Polym. Sci. Part A: Polym. Chem.* **2011**, *49*, 1856–1864.
106 T. M. Eggenhuisen, C. R. Becer, M. W. M. Fijten, R. Eckardt, R. Hoogenboom, U. S. Schubert, *Macromolecules* **2008**, *41*, 5132-5140.
107 D. B. Thomas, A. J. Convertine, L. J. Myrick, C. W. Scales, A. E. Smith, A. B. Lowe, Y. A. Vasilieva, N. Ayres, C. L. McCormick, *Macromolecules* **2004**, *37*, 8941-8950.
108 A. Yamazaki, J. M. Song, F. M. Winnik, J. L. Brash, *Macromolecules* **1998**, *31*, 109-115.
109 S. Ito, *Kobunshi Ronbunshu* **1990**, *47*, 467-474.
110 J. Vinas, N. Chagneux, D. Gigmes, T. Trimaille, A. Favier, D. Bertin, *Polymer* **2008**, *49*, 3639-3647.
111 J. M. Cariou, J. Dugas, L. Martin, P. Michel, *Appl. Opt.* **1986**, *25*, 334-336.
112 P. B. Zetterlund, Y. Saka, R. McHale, T. Nakamura, F. Aldabbagh, M. Okubo, *Polymer* **2006**, *47*, 7900-7908.
113 B. Lessard, C. Tervo, M. Maric, *Macromol. React. Eng.* **2009**, *3*, 245-256.
114 C. Dire, B. Charleux, S. Magnet, L. Couvreur, *Macromolecules* **2007**, *40*, 1897-1903.
115 C. Magee, Y. Sugihara, P. B. Zetterlund, F. Aldabbagh, *Polym. Chem.* **2014**, *5*, 2259-2265.
116 D. Benoit, V. Chaplinski, R. Braslau, C. J. Hawker, *J. Am. Chem. Soc.* **1999**, *121*, 3904-3920.
117 S. Marque, C. Le Mercier, P. Tordo, H. Fischer, *Macromolecules* **2000**, *33*, 4403-4410.
118 F. Chauvin, P. E. Dufils, D. Gigmes, Y. Guillaneuf, S. R. A. Marque, P. Tordo, D. Bertin, *Macromolecules* **2006**, *39*, 5238-5250.
119 T. Schulte, K. O. Siegenthaler, H. Luftmann, M. Letzel, A. Studer, *Macromolecules* **2005**, *38*, 6833-6840.
120 G. Moad, E. Rizzardo, S. H. Thang, *Aust. J. Chem.* **2005**, *58*, 379-410.
121 V. Butun, S. P. Armes, N. C. Billingham, *Polymer* **2001**, *42*, 5993-6008.
122 B. H. Lessard, X. Savelyeva, M. Maric, *Polymer* **2012**, *53*, 5649-5656.

123 J.-F. Lutz, A. Hoth, *Macromolecules* **2005**, *39*, 893-896.
124 G. Delaittre, J. Rieger, B. Charleux, *Macromolecules* **2011**, *44*, 462-470.